

POLITECNICO DI TORINO

Master Degree Course in Electronic Engineering

Master Degree Thesis

Developing and Improving Hardware and Firmware of a Smart Device
Able to Perform an Accurate Diagnosis of Lead-Acid Batteries for
Automotive Applications



Advisor

Prof. Marcello Chiaberge

Candidate

Servan Tursak

Internship Tutor

Eng. Giovanni Guida

March 2021

*I dedicate this thesis to my beloved family
for their endless love and comforting support*

Summary

Since nowadays, especially in the automotive field, lead-acid batteries are getting more important, a good diagnostic of the batteries is becoming essential.

The aim of this thesis work is to develop and improve the hardware and the firmware designs of a smart device that is developed before as a research prototype. The whole purpose of this thesis work is to acquire the necessary parameters, such as voltage, current, temperature, etc. in order to calculate an accurate estimation of SoC (State of Charge) and SoH (State of Health) and send them to a smart central device through Bluetooth using BLE (Bluetooth Low Energy) protocol.

The voltage of the terminals of the battery is measured using a negative feedback amplifier after using a proper voltage divider to have a proper voltage range for the operational amplifier itself. The analog value is acquired through the analog pins of the microcontroller utilizing its own ADC (Analog to Digital Converter).

The current of the battery is also measured by using a Shunt Resistor of 50 micro ohms. For this purpose, the idea is basically first to measure the voltage drop across the terminals of the shunt resistor and then convert it to the current by a firmware algorithm. In order to measure the voltage difference across the shunt resistance, a differential amplifier is utilized since it has a simple design and good gain efficiency. After using the differential amplifier and after amplifying the voltage drop, the data is fed to the analog pins and ADC of the microcontroller.

After having the necessary parameters acquired, they need to be sent to a smart device by using the BLE protocol. For this purpose, application-specific Service and Characteristic creations were necessary. Using an online tool developed by Texas Instruments, some pieces of code are generated and embedded inside the firmware of the design. At that point, the acquired parameters are sent to the central Bluetooth device and monitored by checking the specific area of the created Service and Characteristics.

Since the company has decided not to build the hardware design due to Covid and economical situations, the related firmware is tested on a Launchpad that has exactly the same microcontroller and the required drivers, such as timer and ADC. After flashing the firmware onto the Launchpad, the results on the smart device screen are checked by using the BLE Scanner application. The voltage and the current values are tested at the minimum and maximum points and the results were satisfactory.

For future development, since the hardware design includes a flash memory inside, the offline measuring can be applied. That would be very useful when considering that not always have a Bluetooth connection. The results can be stored inside the flash memory and then once the user connects the device to Bluetooth, the acquired results can be monitored then.

Also as an important point, Cloud Computing can be considered for this thesis work. Since it allows us to connect many devices from many different users, it will make the estimations of the SoC and SoH much accurate.

This thesis work has a big potential to serve as a real industrial solution since it is a complete project with both hardware and firmware designs. Especially when considering that we are in a transition phase from fuel vehicles to electric vehicles, this work can be well utilized for battery diagnostics which will be crucial in the future more than it is now.

Acknowledgments

I would first like to thank my thesis advisor Prof. Marcello Chiaberge. Since my thesis studies coincide with the terrible Covid 19 period, I was in serious doubt whether I can complete my thesis or not. However, Prof. Marcello Chiaberge was so open-minded and understanding that I did not even doubt a second after meeting him. Even though we could not meet face-to-face regularly, due to Covid 19 period, we perfectly communicated online without a single problem. He always steered me in the correct direction whenever I seem to need it. Frankly, I do not think that I could ever find an advisor better than him.

I would also like to thank my tutor Eng. Giovanni Guida, who is working for *brainTechnologies*. He has always been indulgent towards me. If I have learned anything during my thesis period that is worth knowing, huge credit must go to him. He provided almost all the technical tools for me to improve myself and write my thesis. Not only has he guided me about the related technical issues, but also he has shown me that he is a good friend who is there for me to cheer me up even when I am down. He has always been willing for further learning and improvement, which eventually, I believe, made me a better engineer. I can wish nothing but a successful and happy life to him, for he certainly does deserve it.

Finally, I have to express my profound gratitude to my beloved family for their unfailing love, support, and encouragement throughout many years of studying and writing this thesis. Even if it was so hard to stay apart from them, knowing their continuous care and understanding towards me always led me to feel like they were still by my side. There is no word for me to express my appreciation and love for them. My thesis process would not be accomplished without them. Thank you.

Contents

List of Figures.....	viii
List of Table	x
CHAPTER I	1
1. Introduction.....	1
1.1. Concerning Batteries	2
1.1.1. Lead-Acid Batteries	2
1.1.2. Battery Models	3
1.2. SoC and SoH.....	7
1.2.1. Voltage Method	7
1.2.2. Kalman Filter Method	8
1.2.3. Coulomb Counting Method	9
1.2.4. Enhanced Coulomb Counting Algorithm	10
1.3. SoA.....	13
CHAPTER II.....	16
2. HW Implementation	16
2.1. Task Analysis	17
2.1.1. Executive Summary	17
2.1.2. Current Sensing Methods	18
2.1.2.1. Hall Effect Sensor	19
2.1.2.2. Resistive Current Sensing	22
2.1.2.3. Current Sensing Topology Comparison	25
2.1.3. Conditioning Circuitry	26
2.2. Implementation	28
2.2.1. Components.....	28
2.2.1.1. Protection Circuit.....	28
2.2.1.2. Voltage Regulator.....	32
2.2.1.3. Current and Voltage Sensing.....	38
2.2.1.4. Shunt Resistor	46
2.2.1.5. Temperature Sensors	48

2.2.1.6. Microcontroller	50
2.2.1.7. Antenna.....	52
2.2.2. Schematic Explanation	56
2.2.2.1. Voltage Transient Protection Circuit	59
2.2.2.2. Buck Converter	60
2.2.2.3. Microcontroller, XTALs and Antenna.....	61
2.2.2.4. Decoupling	62
2.2.2.5. Current and Voltage Measuring Circuitry	64
2.2.2.6. Board Temperature Sensor.....	65
2.2.2.7. Hood Temperature Sensor	66
2.2.3. Layout Explanation.....	67
2.2.4. Bill of Materials.....	71
CHAPTER III.....	72
3. FW Implementation	72
3.1. RTOS.....	73
3.2. TI-RTOS.....	75
3.3. Peripheral Management.....	76
3.4. Main Program Development	79
3.4.1. Project Zero	79
3.4.2. Sensor Controller Interface	81
3.4.3. Bluetooth Management	82
CHAPTER IV.....	87
4. Verification of FW	87
4.1. CC2640R2 Launchpad	88
CHAPTER V.....	95
5. Conclusion.....	95
5.1. Future Perspectives	96
5.1.1. HW Improvements	96
5.1.2. FW Improvements	98
5.1.3. Cloud Computing	99
5.2. Conclusion.....	100
Bibliography.....	102

List of Figures

Figure 1. 1	Randle’s EECM to model battery impedance response	4
Figure 1. 2	m-th order battery EECM	5
Figure 1. 3	Thevenin Equivalent Model of the Battery	8
Figure 1. 4	Flowchart of the Enhanced Coulomb Counting Algorithm [7]	12
Figure 1. 5	HELLA Intelligent battery sensor (IBS) [9]	13
Figure 1. 6	BOSCH EBS (Electronic Battery Sensor) [8]	14
Figure 1. 7	CONTINENTAL IBS (Intelligent Battery Sensor) [10]	15
Figure 2. 1	Structure of free-Space Hall-effect current sensor	20
Figure 2. 2	High side current measurement [13]	22
Figure 2. 3	Low side current measurement [13]	23
Figure 2. 4	The basic differential amplifier opamp model	27
Figure 2. 5	The whole protection circuitry	28
Figure 2. 6	Operating zones of a TSV diode [15]	29
Figure 2. 7	Operating zones of a MOSFET [16]	30
Figure 2. 8	Physical representation of the P-channel MOSFET	31
Figure 2. 9	Absolute Maximum Ratings of the MOSFET	31
Figure 2. 10	Comparison between Linear and Switching Regulators [17]	32
Figure 2. 11	LMR16006XDDCR pinout [18]	33
Figure 2. 12	Absolute maximum ratings of LMR16006XDDCR [18]	34
Figure 2. 13	Example application circuit of LMR16006XDDCR [18]	34
Figure 2. 14	INA226-Q1 pinouts [19]	40
Figure 2. 15	Current and Voltage Measuring Circuitry	41
Figure 2. 16	Ideal negative-feedback amplifier	43
Figure 2. 17	Op-amp differential amplifier	44
Figure 2. 18	WSBM8518 Resistor with its Package and Molex Connector [24]	47
Figure 2. 19	TMP112x family Digital Temperature Sensor	48
Figure 2. 20	Absolute maximum ratings of TMP112A	49
Figure 2. 21	Electrical characteristics of TMP112A	49
Figure 2. 22	CC2640R2F-Q1 pinout	50
Figure 2. 23	CC2640R2F-Q1 functional block diagram [25]	51
Figure 2. 24	2450AT18A100E 2.4 GHz Mini Antenna	54
Figure 2. 25	2450AT18A100 antenna general specs [27]	55
Figure 2. 26	2450AT18A100 mechanical dimensions [27]	55
Figure 2. 27	Voltage Transient Protection Circuit	59
Figure 2. 28	Buck Converter	60
Figure 2. 29	Microcontroller, XTALs, and Antenna	61
Figure 2. 30	VDDS Decoupling	62

Figure 2. 31	VDDR Decoupling	63
Figure 2. 32	Current and Voltage Measuring Circuitry	64
Figure 2. 33	Board Temperature Sensor	65
Figure 2. 34	Hood Temperature Sensor	66
Figure 2. 35	PCB Layout	67
Figure 2. 36	Antenna and the matching circuit components	68
Figure 2. 37	Top View	70
Figure 2. 38	Bottom View	70
Figure 3. 1	Structure analysis from non-OS to RTOS [28]	74
Figure 3. 2	TI-RTOS Hierarchical Structure [11]	75
Figure 4. 1	TI CC2640R2 Launchpad	88
Figure 4. 2	Pinout of the CC2640R2 Launchpad [30]	89
Figure 4. 3	BLE Scanner app – Custom Service 0xBABE	92
Figure 4. 4	BLE Scanner – Voltage Char 0xBEEF - 0V check.....	93
Figure 4. 5	BLE Scanner - Voltage Char 0xBEEF – 3.3V check.....	94
Figure 5. 1	High-Side Current Sensing with Improved Transient Immunity [31].	96
Figure 5. 2	Cloud computing connecting many stations	99
Figure 5. 3	3D top view	100
Figure 5. 4	3D bottom view	100

List of Table

Table 2. 1	Current load of cars [11]	18
Table 2. 2	Difference between Resistive and Hall Effect current sensing [14]	25
Table 2. 3	Comparison Among different sense amplifiers [11]	39
Table 2. 4	Bill of Materials with the prices of Mouser Electronics Inc.	71

CHAPTER I

1. Introduction

1.1. Concerning Batteries

1.1.1. Lead-Acid Batteries

The lead-acid batteries that Gaston Planté developed in 1859 are the earliest form of rechargeable battery. It is a known fact, of course, that they have a low ratio of energy to weight and energy to volume. However, due to their ability to provide strong surge currents, they have a substantial power-to-weight proportion. Considering their low cost, they are also commonly used to provide the high current provided by starter motors in motor vehicles. While higher energy densities may be provided by certain other battery designs, lead-acid batteries are necessarily selected for practical use, largely because of their low cost relative to current battery technologies and their recyclability.

The lead-acid batteries are generally composed of lead plates inside the sulfuric acid, which is a liquid concentrate, and they are enclosed in a polymer case. The plates can be of different thicknesses depending on the actual purpose of the battery usage. It is also worth mentioning the separators between the anode and the cathode of the battery. In the batteries of type liquid electrolyte, a separator is very crucial. The separator is an accessible lamination that is in between the anode and cathode of a battery, and the primary function of the separator is to prevent the electrical short circuits by keeping the two electrodes as separated as possible. Also, it allows the moving of the ionic charge carriers that are needed to close the circuit for the current flow in each electromechanical cell [1].

The average voltage of every ordinary lead-acid battery cell is viewed as around 2 V, while the voltage for every cell goes from 1.8 V stacked at full release to 2.10 V in an open circuit at full charge. The float voltage, which is the voltage at which a battery is supported after being wholly energized to keep up the battery limit by repaying oneself release of the actual battery [2], changes relying upon the battery type (for example, overflowed cells, gelled electrolyte, retained glass tangle), and ranges from 1.8 V to 2.27 V. Moreover, the leveling voltage and the charging voltage for the cells range from 2.67 V to around just about 3 V.

1.1.2. Battery Models

As it tends to be valued by the most, batteries are predominantly some electrochemical frameworks with high complexities. Thus, it's anything but a simple assignment to address them as explicit models. There is a wide range of viewpoints and approaches to addressing the batteries as models. Every battery model itself has various attributes altogether, and choosing them relies upon the compromise of two specific measures, to be particular precision and complexity [3].

Electrochemical Models

When it comes to addressing the natural physical electrochemical cycles of batteries, electrochemical models can be exceptionally precise. Notwithstanding, we may require various boundaries identified with the inside and out information on the battery's substance design, precisely the synthetic composition, to utilize the electrochemical models for reproduction. This makes it truly difficult to have decent reasonableness of the frameworks. The previously mentioned boundaries are difficult to get in light of the nature of the battery innovation. Furthermore, to tackle the reliant fractional differential conditions, complex mathematical procedures are expected, prompting overpowering computational cost for on-board frameworks. [4]

Reduced-order Models

An improved reduced-order battery model has been portrayed by methods for some other suspicions, for example, ignoring the strong fixation circulation along the anode and thinking about the material dispersion inside a delegate vital material molecule for every terminal, and brought about a found the median value of battery model. [5]

Due to the previously mentioned suppositions, when compared to the electrochemical models, the decreased request models bring about a substantial loss of data. Nonetheless, they are adequately exact for explicit applications, for example, SoC assessment and voltage forecast, and display a low computational expense that is alluring for real-time usage. [4]

EECMs

EECMs (Equivalent Electrical Circuit Models) consist of electric components, such as resistors, voltage sources, and capacitors. Besides, to model the battery behavior, they might include some non-linear elements, such as Warburg impedance. There are two different types of EECMs.

Impedance based EECMs

In this kind of EECM, the battery impedance is estimated by methods for making an AC current move through the battery, and because of that, the AC voltage reaction is noticed. At that point utilizing an FFT analyzer, the complex impedance of the battery can be determined. The battery's impedance change with the estimation of SoC (State of Charge), temperature, and the direction and amplitude of the DC current, i.e., the working point [6].

As indicated by Randle's equivalent electric circuit, one single battery cell can be displayed in a disentangled manner, as it very well may be seen from Figure 1.1.

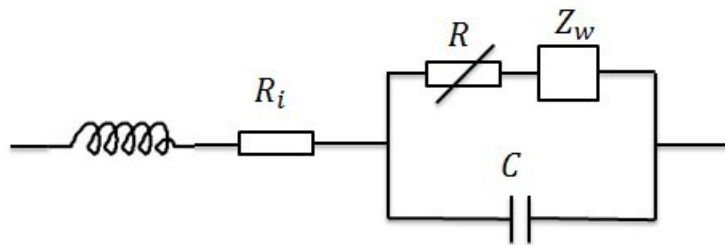


Figure 1. 1 Randle's EECM to model battery impedance response

Voltage-Current based EECMs

The need for a signal generator in order to measure the Electrochemical Impedance Spectroscopy (EIS) of the battery is actually not practical for on-board implementation. Therefore, it has become a common thing to introduce another battery model, taking into consideration the actual existing elements of the onboard elements, such as the voltage, the current, and the temperature.

As referenced above, we may have some non-direct components, for example, Warburg impedance, and as it tends to be valued, its investigation can be mind-boggling. All together keep away from those complexities, a straight EECM is utilized, which comprises of an ideal voltage source, which characterizes the Open Circuit Voltage (OCV), which is constrained by SOC and temperature, a resistor which remains as the internal opposition, and some arrangement RC networks to secure the highlights of the battery. The quantity of RC networks inside the EECM characterizes the order for it. For instance, the EECM is characterized as an n -th request in the event that it is composed of n series RC networks. [4]

The linear behavior of the EECM structure makes it very easy to identify and configure the battery parameters. Furthermore, it does not require to have a knowledge of physical-chemical battery processes, which makes it really easy for the EECM to be applied to different types of batteries. Figure 1.2 shows the typical structure of an m -th order EECM, where v is the terminal voltage, and i is the current.

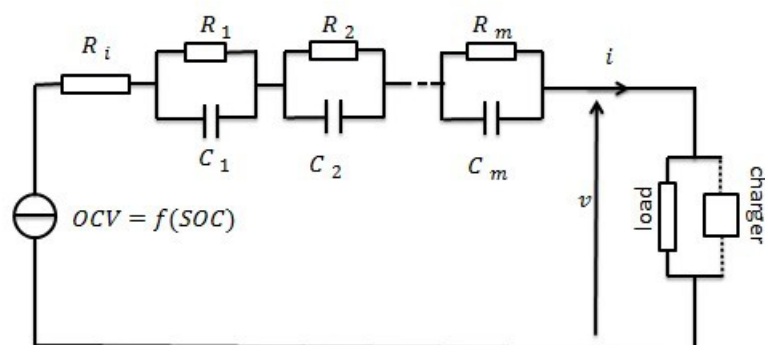


Figure 1.2 m -th order battery EECM

Bio-inspired black-box Models

Black-box models do not require to deal with the physical electrochemical processes of the battery in order to introduce a battery behavior using some intelligent modeling methods.

The consistency of black-box models depends largely on the training data and training method. If the black-box model is chosen to be used, a large number of parameters will be needed to achieve acceptable accuracy.

Hybrid Models

As the name implies, the hybrid model is a combination of both the electrochemical and the RC electric circuit model. While the electrochemical modeling allows robustly estimating of the SoC, including non-linear variations and self-recovery, the RC electric model reproduces a broad spectrum of dynamics.

1.2. SoC and SoH

As explained in the previous part, there are many different ways to model the battery behavior. That leads, of course, to many different ways to define and calculate the SoC (State of Charge) and SoH (State of Health) of the battery under consideration. Those two values are two significant variables that are highly used when a battery analysis is to be made accurately.

The SoC can be easily defined as the available capacity (A/h) and is expressed as a percentage of the rated capacity of the battery. Also, the SoC parameter can be observed as a thermodynamic quantity that can enable the assessment of the potential energy of a battery. [7]

Furthermore, alongside the SoC parameter, it is also essential to estimate the SoH of a battery. SoH basically represents a measurement of the battery's capability to store and deliver electrical energy, compared to a new, fresh battery. [7]

As stated before, there are many ways to calculate the above mentioned SoC and SoH in order to estimate and analyze the features of the battery under consideration. Here, the most known three methods will be discussed, as they are the primary references of this thesis work.

1.2.1. Voltage Method

This method is one of the simplest and basic methods known by many that allow us to calculate and observe the SoC by merely measuring the voltage value of the battery itself. This is known as the discharge test method as well.

However, the measured voltage of the battery is highly affected by the current of the battery, mainly due to the temperature. This, of course, may lead us to observe some wrong results out of the discharge test and eventually to have the wrong SoC. Of course, this drawback can be compensated by adding and adjusting some correctional terms for the battery current. However, the required voltage level stabilization may not be obtained to have a correct and accurate calculation of the SoC. This is the main reason why this method is not easy and accurate to implement.

Another drawback of this method is that the discharge test method, of course, will need consecutive recharging of the battery for acquiring the best outcome out of the test itself. However, this may take very long and time consuming for the desired calculation method in use.

1.2.2. Kalman Filter Method

Kalman Filter Method introduces an algorithm in order to estimate and observe the inner state of any dynamic system. Therefore, it is wise to use it in order to calculate the SoC of the battery as well, since the batteries are dynamic systems themselves.

Kalman filters were first presented in 1960, and their point was to give a recursive answer for the ideal direct separating for both state perception and forecast issues. Remarkably, one of the fantastic sides of utilizing the Kalman filters is that they naturally give some dynamic error bounds on their own state gauges when contrasted with the other assessment draws near. In this way, by displaying the battery framework to incorporate the needed obscure amounts (for example, SoC and SoH) in its state portrayal, the Kalman channel assesses their qualities and gives blunder limits on the evaluations. At that point, it turns into a model-based state assessment strategy that utilizes a blunder adjustment instrument to give continuous forecasts of the SoC. Besides, it tends to be reached out to build the continuous SoH assessment capacity utilizing the all-encompassing Kalman filter. [7]

Not only the Kalman filter method requires a considerably precise model for the battery, but also it requires precise parameter identification as well. The most common model chosen to be used with the Kalman filter is the so-called Thevenin Equivalent Circuit model, as depicted in Figure 1.3.

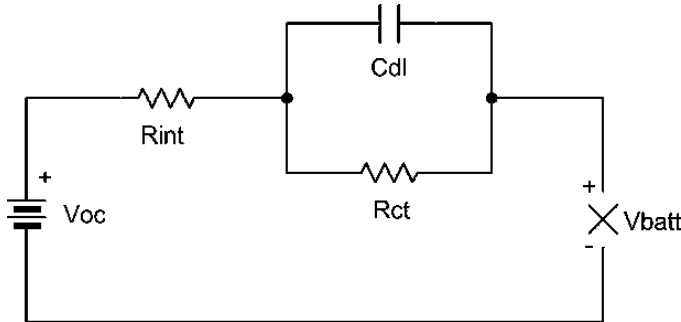


Figure 1.3 Thevenin Equivalent Model of the Battery

1.2.3. Coulomb Counting Method

This method, also known as ampere-hour counting and current integration, is the most used and the most common method to calculate the SoC. In this method, the current readings are integrated over the usage period, given by Formula 1.1 where $SoC(t_0)$ is the initial SoC, C_{rated} is the rated capacity, I_b is the battery current I_{loss} is the current consumed by the loss reactions.

$$SoC = SoC(t_0) + \left(\frac{1}{C_{rated}}\right) \times \int_{t_0}^{t_0+t} (I_b - I_{loss}) dt \quad (1.1)$$

At that point, by aggregating the moved charge of the battery, the Coulomb Counting Method ascertains the leftover charge limit. As it very well may be deducted effectively by noticing the Formula 1.1, the exactness of this technique relies intensely upon the precise and exact estimation and perception of the initial SoC esteem, which implies that with a pre-known battery charge limit, the SoC can undoubtedly be determined by utilizing the Coulomb Counting Method.

Nevertheless, in any case, the releasable charge is not exactly the put-away charge in the charge and release period, which means that losses can occur during the phases of charge and release. Such losses cause accumulating errors, as well as self-discharge. These considerations should be considered for a more reliable SoC evaluation.[7]

1.2.4. Enhanced Coulomb Counting Algorithm

We know that there are some drawbacks to the Coulomb Counting Method. These drawbacks, such as having some shortcomings and poor estimation accuracy, can be overcome by introducing this Enhanced Coulomb Counting Algorithm in order to estimate SoC and SoH of the batteries more accurately.

We can define $C_{\text{releasable}}$ (releasable capacity) as the capacity released when the battery is completely discharged. So the SoC is expressed as the percentage of C_{rated} (rated capacity) divided by $C_{\text{releasable}}$, as can be seen from Formula 1.2 below.

$$SoC = \frac{C_{\text{releasable}}}{C_{\text{rated}}} \times 100\% \quad (1.2)$$

Suppose that we define C_{max} as the maximum releasable capacity of a fully charged battery. However, the C_{max} value is not always fixed. It will continue decreasing as the battery is used more and more. So we can say that the C_{max} value will be different than C_{rated} value as the battery is used, and the percentage of their ratio will give us SoH, as shown by Formula 1.3 below.

$$SoH = \frac{C_{\text{max}}}{C_{\text{rated}}} \times 100\% \quad (1.3)$$

Furthermore, we can define DoD (depth of discharge) as the battery is discharging. It is calculated by the percentage of the capacity that has been discharged relative to C_{rated} as given in Formula 1.4 below.

$$DoD = \frac{C_{\text{released}}}{C_{\text{rated}}} \times 100\% \quad (1.4)$$

Then, as a percentage, we can extract the shift in DoD. The difference between the DoD and the operating time (\mathbb{T}) can be determined using the measured charging and discharge current (I_b) using Formula 1.5 below, where I_b is positive for charging and negative for discharging.

$$\Delta DoD = \frac{-\int_{t_0}^{t_0+\mathbb{T}} I_b(t) dt}{C_{rated}} \times 100\% \quad (1.5)$$

Of course, as time goes on, the value of DoD will be accumulated, as given by the Formula 1.6 below.

$$DoD(t) = DoD(t_0) + \Delta DoD \quad (1.6)$$

Finally, we can express SoC without considering the operating efficiency and the battery aging as given by the Formula 1.7 below.

$$SoC(t) = 100\% - DoD(t) \quad (1.7)$$

Finally, knowing the SoH is not perfect and is not 100%, a relation, given by Formula 1.8 below, can be easily derived between SoC and SoH.

$$SoC(t) = SoH(t) + DoD(t) \quad (1.8)$$

It should be noted that this Enhanced Coulomb Counting Algorithm is totally an online method, which means that the parameters needed to estimate SoC and SoH of the battery by using this method are updated continuously as the battery is used. If we are to consider a new battery, we consider SoH to be equal to 100%, and in order to come up with an initial SoC, the Voltage Method (section 2.1) should be used.

Figure 1.4 below shows the flowchart of the whole Enhanced Coulomb Counting Algorithm, as explained above.

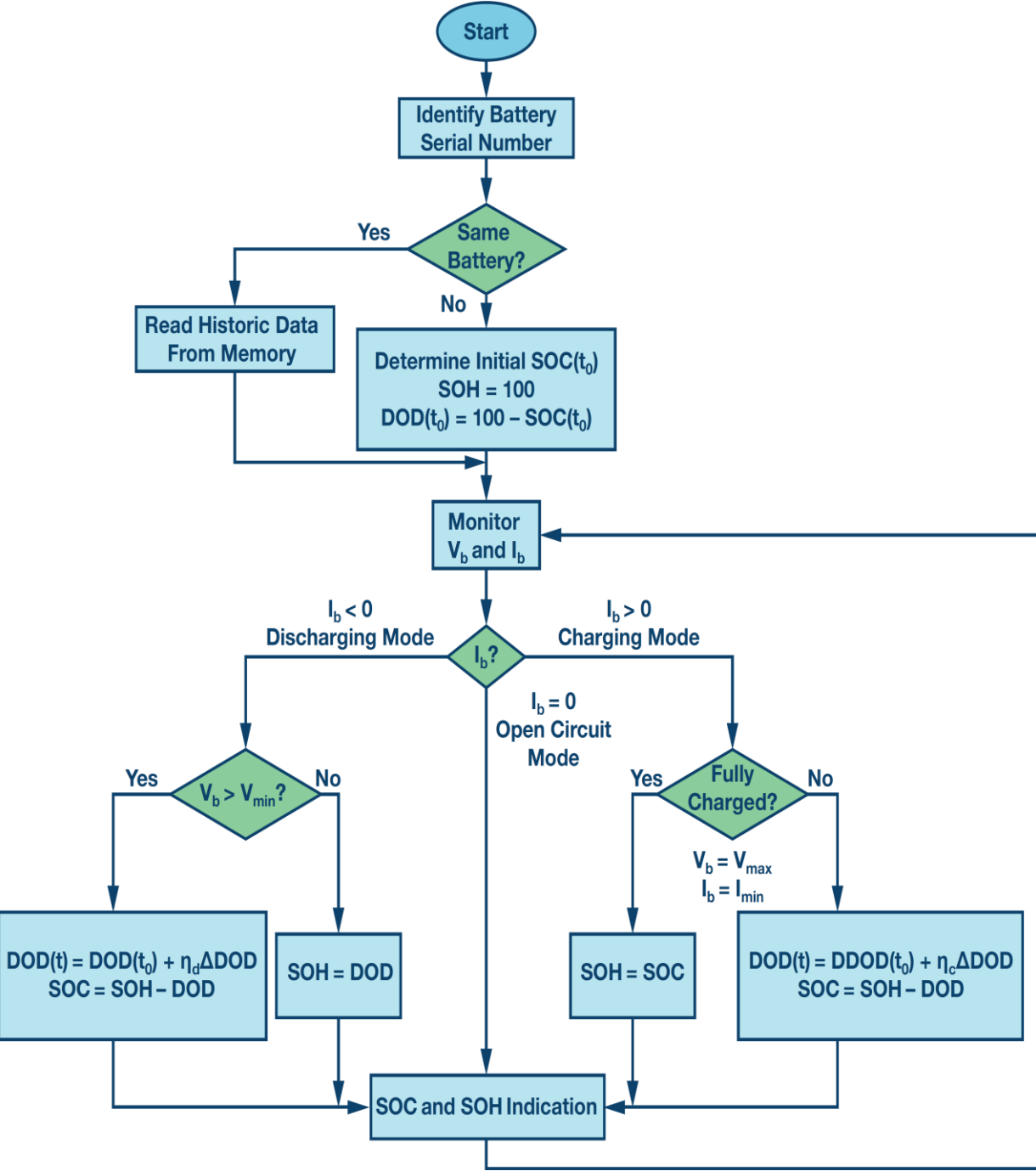


Figure 1. 4 Flowchart of the Enhanced Coulomb Counting Algorithm [7]

1.3. SoA

In this SoA (State of Art) section, some different types of products and devices of the same usage area as the BATMAN device are reported for comparison.

- **HELLA IBS (Intelligent Battery Sensor)**

The IBS dependably and precisely gauges the battery voltage, current, and temperature boundaries. Data on the state of charge (SoC), state of health (SoH), and state of function (SoF) of the battery are determined algorithmically utilizing the estimations. The IBS is intended to be utilized in the starter (standard or EFB), gel, and AGM batteries to screen in-vehicle starter or purchaser batteries. The IBS can be straightforwardly coordinated into the vehicle's electrical framework with the normalized LIN protocol.[8]

The IBS is appended straightforwardly to the negative terminal of the battery. Close by the terminal, the mechanical part of the battery sensor comprises the shunt and grounding bolt. The shunt is joined to the vehicle's heap way and is utilized as an estimating resistor to gauge the current in a roundabout way. The electronic board and the electronic parts are also situated in a cast lodging with a plug connector that capacities as the interface to the energy management framework. The correspondence communication interface utilized is LIN communication, and it interfaces the client to the more elevated level control unit. The stockpile voltage, utilized at the same time as the reference voltage for voltage estimation. [8]



Figure 1.5 HELLA Intelligent battery sensor (IBS) [8]

- **BOSCH EBS (Electronic Battery Sensor)**

The EBS device works on estimating and providing reliable and accurate 12V battery status information. It is also effective considering that it considers the battery's aging while updating its required internal parameters for calculations. Therefore, EBS can give us an implementation of an optimized EEM (Electrical-Power Management System) for the vehicle it is mounted.

Physically, the EBS is connected to the negative terminal of the 12V battery while attached to the car body. It senses the battery voltage, temperature, and also, using a shunt resistor, the current as of the input parameters in order to calculate and provide SoC, SoH, and SoF (State of Function).

Using the estimates reliable SoC parameter, EBS controls the EEM in the central control unit and allows it to regulate the ancillary load in order to optimize the battery life and also the fuel consumption parallelly.

The SoF parameter is used to foresee the effect of the load profile on the battery voltage curve.

Moreover, many other factors can be calculated using the SoH value, such as battery aging and how it affects the battery capacity to store energy and its power output.



Figure 1. 6 BOSCH EBS (Electronic Battery Sensor) [9]

- **CONTINENTAL IBS (Intelligent Battery Sensor)**

A shunt-type device, the IBS device continuously analyzes the status of traditional 12V lead-acid batteries and provides details about the battery's SoC, SoF (power capacity), and SoH (aging).

The IBS is mounted directly from the negative terminal of the battery to the battery, which ensures that it can be placed on any regular 12V battery.

The sensor increases the diagnostic capacity of the car and can also warn of potential breakdowns that may not even be triggered by the battery. In addition, with an enhanced charging strategy, the IBS helps to boost battery life by 10 to 20 percent. [10]

Technical Specifications [10]

1. 5 V - 18 V range of voltage
2. -1500 A - 1500 A range of current
3. 10 % SoC accuracy
4. 10 % SoH accuracy
5. 500 mV SoF accuracy
6. -40 °C - 105 °C of working temperature
7. Using LIN Communication



Figure 1. 7 CONTINENTAL IBS (Intelligent Battery Sensor) [10]

CHAPTER II

2. HW Implementation

2.1. Task Analysis

2.1.1. Executive Summary

The original BATMAN project was started by two engineers, Di Fazio and Fazi, under the tutoring of Prof. Pasero from Politecnico di Torino. [11] Their work is a starting point of this thesis as it stands as a research project for future uses. However, this thesis aims to improve the original project and make it an accurate and real industrial solution by modifying and improving both the hardware and the firmware designs.

The BATMAN project itself aims to provide accurate SoC and SoH values of different types of lead-acid batteries it is connected to while standing out as being low-cost and easy to apply the product. In order to achieve before mentioned purposes, it has to have some specific features.

Firstly, as we all know, the BATMAN product's work area is really prone to be malfunctioning in terms of distorted values of SoC and SoH, mainly because we are handling such tiny voltage and ampere values. The product should avoid some dangerous service malfunctions by knowing the critical states it may be.

Furthermore, it should acquire and sense the correct parameters in order to calculate and provide the necessary SoC and SoH utilizing solid hardware and firmware design.

Then, of course, it should have an interface that allows a user, or any other system, the calculated accurate SoC and SoH values so that the possible necessary actions on the battery can be taken.

Also, taking into account that this device is to be out in the market, it should be available for both in-market and after-market productions. So it should have a PCB to which the concerning battery is to be connected in order to provide the necessary parameters.

The device should not only acquire the parameters for SoC and SoH calculations, but it should also send the data to a user interface platform with solid precision. For this purpose, it should embrace a BLE (Bluetooth Low Energy) communication protocol. The platform with which the user interacts with the calculated and sent data should be an application available to smartphones or tablets.

2.1.2. Current Sensing Methods

As it can be appreciated, acquiring an accurate SoC and SoH depends on the accuracy and variety of the necessary parameters. Most of the devices and products out in the market use voltage measurement in order to estimate SoC and SoH. It is indeed a beneficial and easy way to observe the battery stats. However, it is not enough to get an accurate SoC and SoH by itself. That is the reason why using the current measurement as another parameter in calculating battery stats seems to be very useful and leads us to have a more intelligent algorithm.

However, it is not an easy task to deal with high current values, as this is the case for many of our target batteries. Since we are mainly focusing on car batteries, it can be wise to estimate the amount of current a vehicle consumes. Table 2.1 below shows the approximated values of currents of each piece of equipment of the vehicle.

Equipment	Current Sank
Ignition	2-9A
Radio	0.5-5A
Windshield Wipers	7.5A
Headlamps (Low Beam, Dim)	17-18A
Headlamps (High Beam, Bright)	19-20A
Parking lights	4-10A
Brake lights	6-11A
Interior lights	2-4A
Bonnet Light	0.5-1A
Horn	4A
Power Window (One window)	5A
ABS Brakes (Max)	14A
Boot Light	0.5-1A
Blower (Heater, Air Conditioner)	10-14A
Heated Rear Window Defogger	13-28A
Heated Seat	4-5A
Power Seat Motor	10-13A
Summer Starting (Petrol)	150-200A
Summer Starting (Diesel)	450-550A
Winter Starting (Petrol)	250-350A
Winter Starting (Diesel)	700-800A

Table 2.1 Current load of cars [11]

In order to avoid unexpected system failures, the worst-case scenario is considered, and according to that consideration, the maximum current load is assumed to be approximately 1000A. That leads us to consider a functional current sensing circuitry out of different current sensing topologies.

The two of the main current sensing ways used by the many are Hall Effect Sensor and Resistive Current Sensing, that is listed below alongside their pros and cons at the end of each discussion.

2.1.2.1. Hall Effect Sensor

The Hall Effect Sensors are utilized as non-contact advances dependent on the rule that for a given current stream, a relative magnetic field is delivered around the current-conveying conductor. The general design can be found in Figure 2.1 below.

There are three essential parts of the Corridor impact sensors; the core, the Hall effect gadget, and the comparing signal conditioning hardware.

The core is magnetically permeable, and it focuses on the conductor's magnetic field. The Hall effect gadget is deliberately mounted in a slight cut in the core, at a correct point to the concentrated attractive field, and a steady current energizes it. When the Hall gadget is empowered, it gets presented to a magnetic field from the core. Afterward, it delivers a potential difference that can be estimated and enhanced into measure level signals, for example, 4-20mA or a contact conclusion.[12]

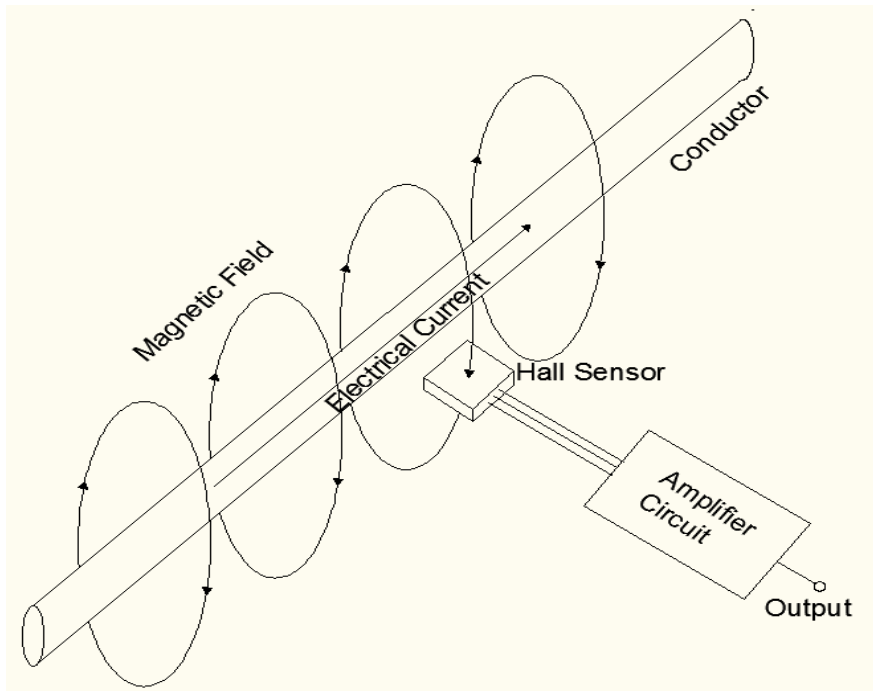


Figure 2. 1 Structure of free-Space Hall-effect current sensor

Since the task of this thesis is not to explain different current sensing topologies in deeper details, here, only the Free-Space Current Sensing topology based on the Hall Effect Method is further discussed.

This method, of course, is tough to apply on real systems such as BATMAN because of the dependency of the distance between the actual sensor and the wire it is placed near, as it can be more explicit by below Formula 2.1.

$$B = \frac{\mu_0 I}{2\pi r} \quad (2.1)$$

Where;

B is the induced magnetic field

I is the flowing current through the wire

μ_0 is the magnetic permeability of the air

r is the distance from the conductor to the sensor

The other worth mentioning lousy side of this method is that it is heavily affected by the magnetic field of the Earth itself. Because of this effect, the result of this method will depend on the spatial orientation of the sensor. [11]

The pros and cons of the Hall effect sensor method are listed below.

Pros:

- It can support high-speed operations over 100 kHz
- Since it is a non-contact operation, there is no wear and friction. Hence it leads to having the possibility for an unlimited number of operating cycles
- Its magnetic offset can be compensated anytime
- It has a good precision
- It is capable of measuring large currents

Cons:

- Its temperature rating is minimal
- It is highly susceptible to EM (Electromagnetic) disturbances
- Magnetic offset due to core magnetization
- The electrical offset can be affected by temperature
- In order to avoid the noise problems, modulation may be needed
- It has a non-linear behavior with respect to temperature
- Its calibration process is comparably difficult

2.1.2.2. Resistive Current Sensing

This method involves adding a shunt resistor in series with the load. The resistive current sensing approach is the most commonly used technique, and it is straightforward to use.

By putting the shunt resistor in series with the load, the voltage drop across the shunt resistor is measured according to the current flowing through it by the source. After measuring the voltage drop across the two terminals of the shunt resistor, we can simply switch to the current by applying the Ohm's Law, as stated in Formula 2.2, where I is the current flowing through the shunt resistor, V is the voltage drop across the shunt resistor, and R is simply the value of the shunt resistor.

$$I = \frac{V}{R} \quad (2.2)$$

The insertion of the shunt resistor can be applied in two different ways. Simply, it can be put either before or after the load, respectively called as high side and low side current measuring, as it can be seen from Figure 2.2 and Figure 2.3 below.

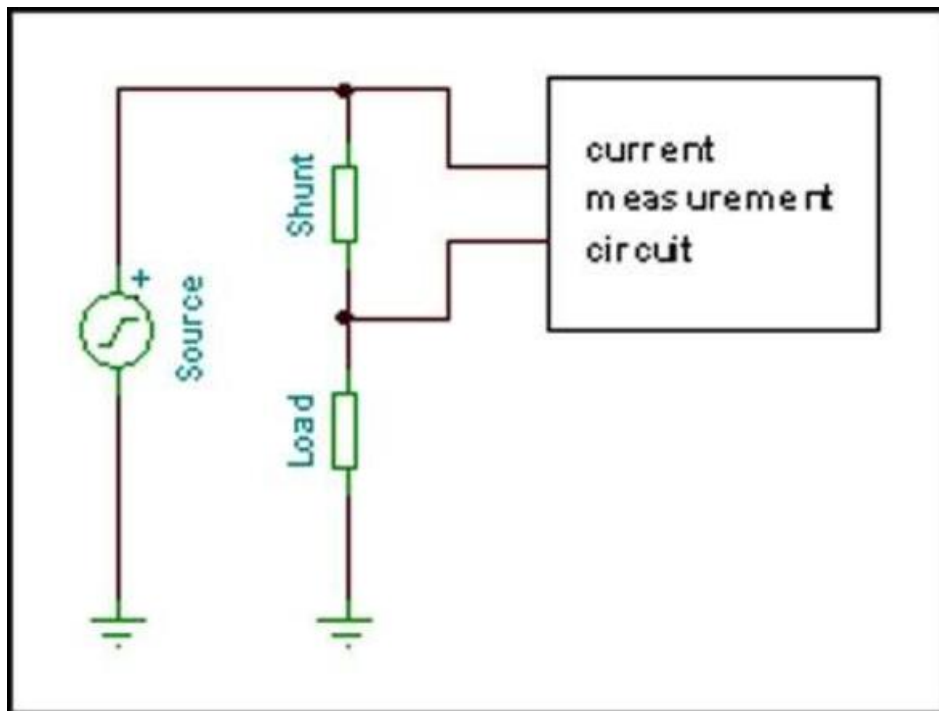


Figure 2.2 High side current measurement [13]

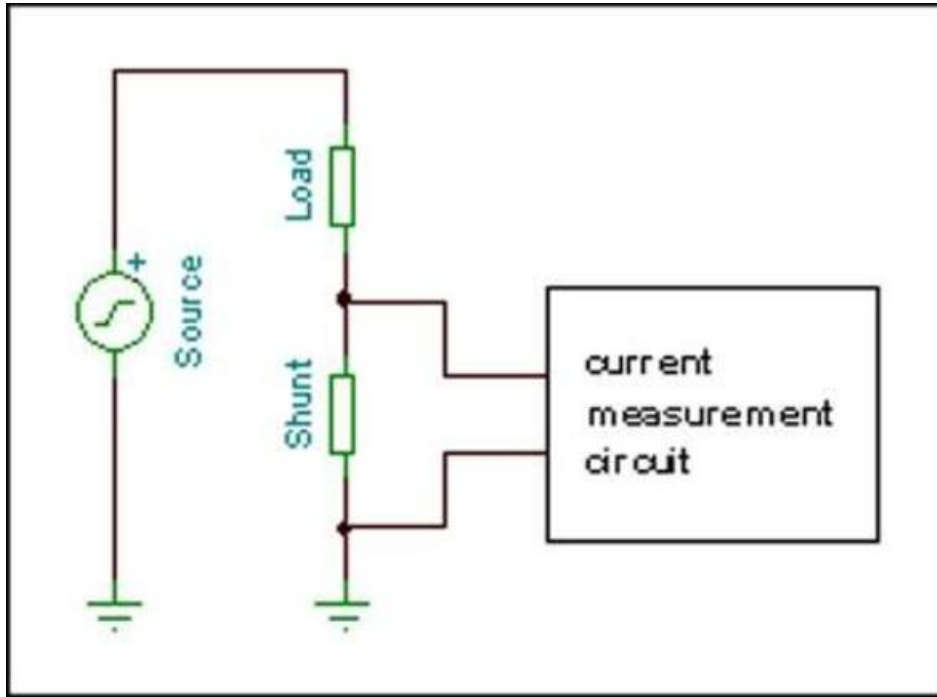


Figure 2. 3 Low side current measurement [13]

We know that while trying to apply and implement a component into an electrical board, it is essential that we have a good range of flexibility on them. One of the most flexible components out there is resistors, as they can be of different formats, values, power ratings, accuracies, etc. That is the reason for choosing this method in the project. However, there are, of course, some drawbacks of this method. Since we are applying the shunt resistor in series, it becomes quite challenging to implement that idea on an existing device. Furthermore, this method will imply that the electrical components that are responsible for measurement are not electrically insulated at all. However, this drawback can be neglected for human safety as the only relevant parameter for electrical isolation is voltage, not current.

Since we are introducing a new resistance to the power source, the voltage delivered to the load must be as similar as possible to the source one to guarantee the proper behavior of the system. So, there is an essential trade-off between having a high current measurement precision and a low voltage drop across the resistor. [11]

The pros and cons of the resistive current sensing method are listed below.

Pros:

- Its temperature rating is very high
- The shunt resistor offers a very flexible design with many formats, values, power ratings, accuracy, and material available
- The system is highly robust to EM disturbances
- It has a great precision
- It has a comparably low noise
- It has a wide dynamic range

Cons:

- There is a lack of electrical insulation
- It introduces additional parasitic inductance
- It dissipates comparably more power
- It is difficult to be applied to the existing systems

2.1.2.3. Current Sensing Topology Comparison

In the light of the above-mentioned pros and cons of the two different current sensing approaches, a decision is to be made for the BATMAN project.

A detailed comparison between the two approaches is listed in Table 2.2 below.

CATEGORY	SHUNT-BASED	HALL-BASED
Solution size	Similar	Similar
Offset	Very Low	Medium
Offset drift over temperature	Low	Medium
Accuracy	<0.5% after calibration	<2% after calibration
Noise	Very Low	High
Bandwidth	Similar	Similar
Latency	Similar	Similar
Nonlinearity	Very Low	High
Long-term stability	Very High	Medium
Cost	Similar	Similar
Vibration Impact	Very Low	Low
Power dissipation	Low	Very Low
Customization	Flexible	Limited

Table 2. 2 Difference between Resistive and Hall Effect current sensing [14]

The Hall effect sensor approach would not be a good solution for our problem, mainly due to the fact that it is highly affected and distorted by the external EM disturbances. Apart from that, we have also mentioned that its temperature ratings are deficient. The maximum temperature for the Hall effect sensor would be approximately 85°C , which can be counted as a low value when considering that the main working area of the device will be automotive vehicles, of which temperature rating is not less than 105°C . [11]

However, the shunt resistor approach can be a good solution for our problem. As mentioned in the pros and cons section of its own, it is really robust towards the external EM disturbances, it has a linear topology, and it introduces a comparably low noise. This method is chosen for this project as it would be wise to do so.

2.1.3. Conditioning Circuitry

Since a shunt resistor will be used in the design in order to measure the current, a suitable conditioning circuitry is needed in order to acquire the needed voltage correctly.

Knowing that the shunt resistor is placed in series in between the source and the load, it, of course, should have significantly low resistance (around $50\mu\Omega$) values in order to avoid high potential difference drops and by doing so, maintaining the correct behavior of the system.

Many battery feature measurement devices on the market use various commercial integrated components that are able to acquire both the voltage and the current by utilizing the component's own ADC (Analog to Digital Converter) to convert the acquired analog value to digital bits.

This is very common for many devices, and it may give some satisfying results. However, that solution is quite expensive in terms of cost and also occupies a lot of area in the related PCB (Printed Circuit Board). Having an intelligent microcontroller in the system, it may sound unnecessary to use another integrated component's ADC.

This is the reason why we have decided to use another approach to get the required current value. A simple and effective differential amplifier is used in the project.

The input terminals of the differential amplifier are connected to each side of the shunt resistor in order to measure the voltage drop across it. Then, of course, it amplifies that voltage difference in order for the microcontroller to sense the value correctly since the voltage drop across the shunt resistor will be very low in order not to affect the system itself. The whole conditioning circuitry is summarized in the simplified Figure 2.4.

Basic differential amplifier op amp model

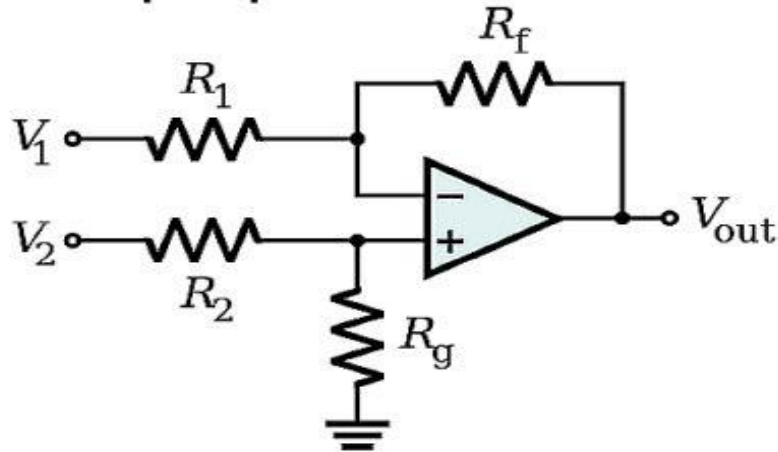


Figure 2. 4 The basic differential amplifier opamp model

Where V_1 and V_2 are connected to the terminals of the shunt resistor in order to measure the voltage difference across it.

This configuration basically senses the voltage difference between the terminals of the shunt resistor and amplifies it according to its gain, which can be seen in the Formula 2.3 below.

$$V_{out} = \frac{(R_f + R_1)R_g}{(R_g + R_2)R_1} V_2 - \frac{R_f}{R_1} V_1 \quad (2.3)$$

In the above Formula 2.3, if we consider $R_1 = R_2$ and $R_f = R_g$ as this is the most common method in the literature, it becomes as the Formula 2.4 below.

$$V_{out} = \frac{R_f}{R_1} (V_2 - V_1) \quad (2.4)$$

Then, of course, after amplifying the slight voltage difference by the gain, calculated by the above formula, and since we know the exact value of the shunt resistor, we can simply switch to the current value because we correctly obtained the voltage drop across its terminals.

2.2. Implementation

In the light of the above-mentioned specifications and targets, the next step is to implement the components physically and design the electronic board PCB according to it.

2.2.1. Components

2.2.1.1. Protection Circuit

When dealing with such high voltage and current values on a single board, the protection circuitry is a must to have in order not to damage the board itself and hence not to disorient the correct working behavior of the system.

The complete protection circuit is given in Figure 2.5 below.

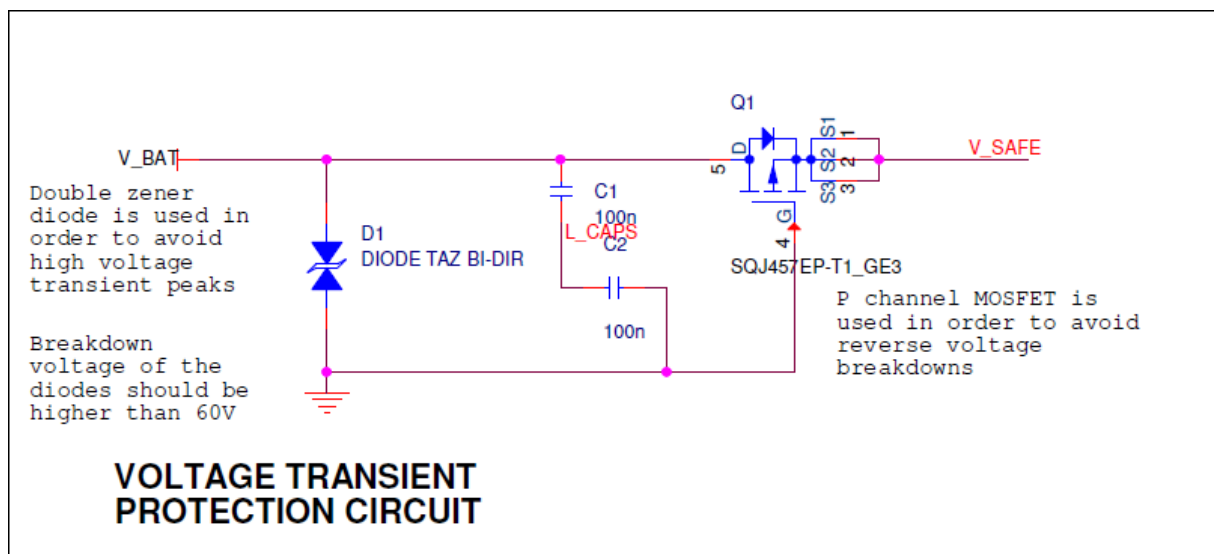


Figure 2. 5 The whole protection circuitry

The protection circuitry used in this project consists of two main phenomena. The first one is to use a Zener diode as a TSV (Transient Voltage Suppressor) circuit, and the other one is to use a MOSFET to avoid reverse voltage breakdowns.

- **TSV Diode**

The transient voltage suppressor is very common to use for basically suppressing the transient coupling voltages according to the ISO7637-3 standard.

This avoids two types of coupling effects, namely the capacitive and inductive couplings. For this action, a Transzorb diode is used. For a quick conceptual understanding, Figure 2.6 below shows the operating zones of a TVS diode.

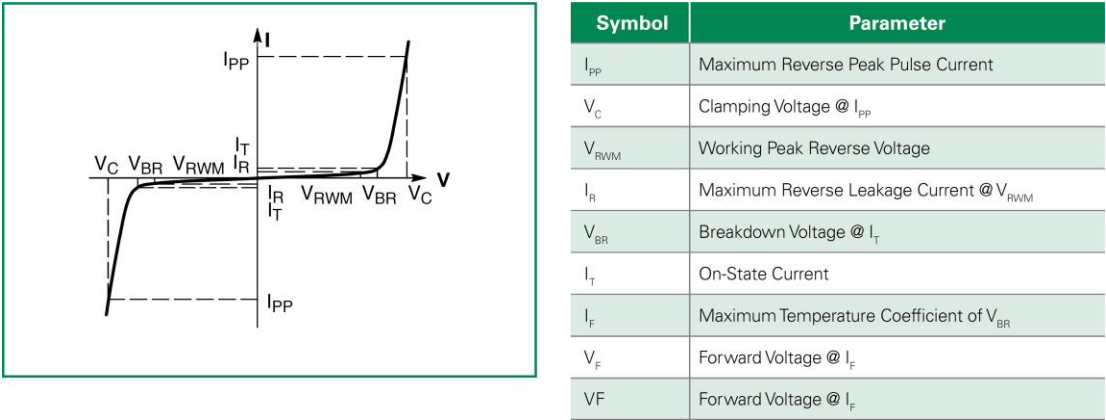


Figure 2. 6 Operating zones of a TSV diode [15]

For our case, since the design should be dealing with voltages up to 60 V, the breakdown voltage V_{BR} should be at least 60 V in order to maintain healthy system protection. The specifications of the TSV diode used are listed below.

- Reverse Standoff Voltage V_R is 64 V
- Minimum Breakdown Voltage V_{BRmin} (I_T (test current) of 1 mA) is 71.10 V
- Maximum Breakdown Voltage V_{BRmax} (I_T (test current) of 1 mA) is 78.60 V
- Maximum Clamping Voltage V_C is 103.0 V
- Maximum Peak Pulse Current I_{PP} is 3.9 A
- Maximum Reverse Leakage Current I_R is 1 μ A

- **MOSFET**

This type of protection is needed for reverse voltage breakdowns. Suppose that a user connected the battery in the reverse way than it should be. This would cause a reverse voltage running through the board, and this may damage the whole system if without proper protection against it.

We use a P-channel MOSFET in order to avoid these kinds of reverse voltage effects. What it does basically is that when the source is connected in a correct way, it behaves like a closed switch, and it allows the current to pass through the system. However, when the voltage is reversed, the MOSFET will lock itself and will not allow any voltage potential occurrences through the system; hence it protects the system from these types of situations.

For further information, the operating principles of a MOSFET are illustrated in Figure 2.7 below.

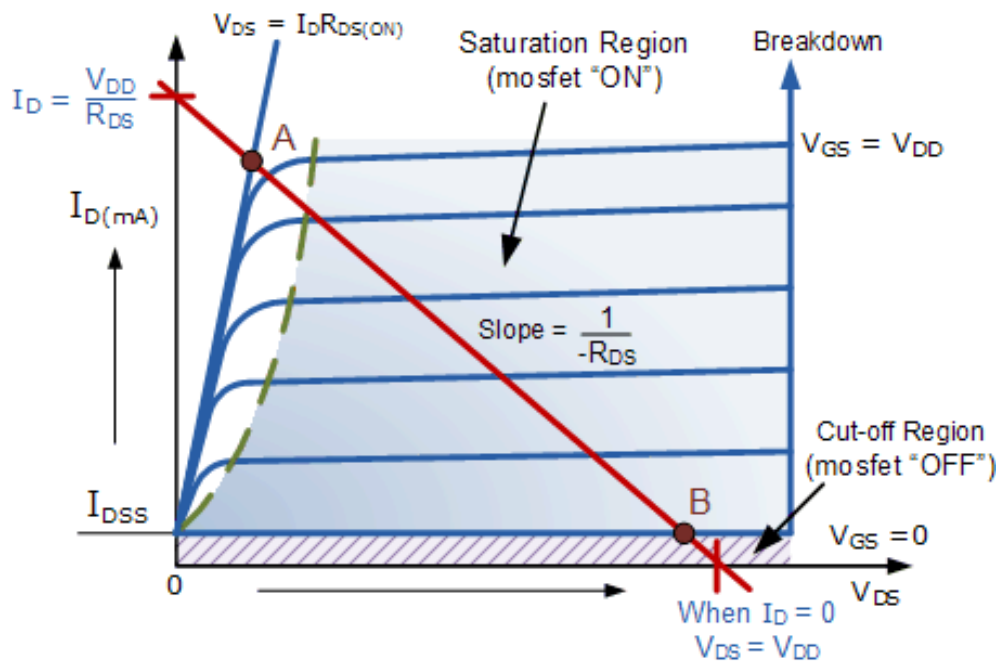


Figure 2.7 Operating zones of a MOSFET [16]

The MOSFET is an excellent idea in terms of reverse voltage breakdown usage because not only it locks the reverse voltage, but also it introduces a very low resistance, which is pretty desired in the systems such as ours in order not to change the required voltage values applied to the system itself.

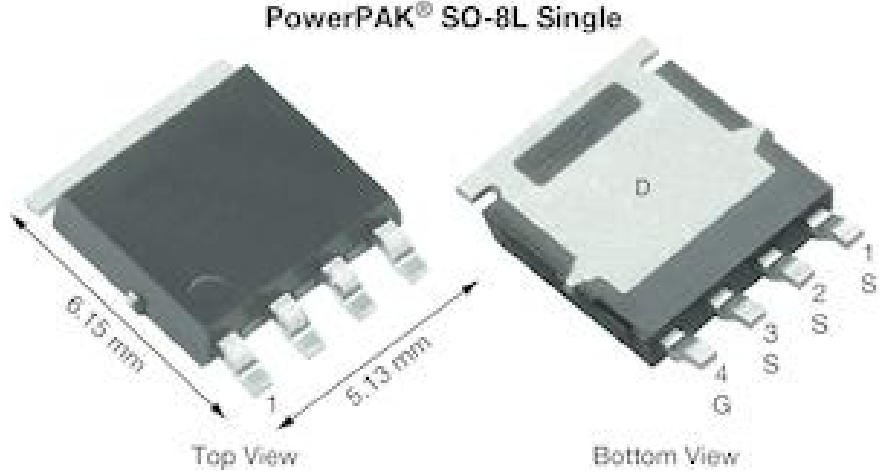


Figure 2.8 Physical representation of the P-channel MOSFET

The MOSFET we will use, illustrated in Figure 2.8 above, has the following characteristics.

- Drain to Source voltage V_{DS} is -60 V
- Drain to Source on-resistance R_{DSon} (at $V_{GS} = -10$ V) is 25 m Ω
- Drain to Source on-resistance R_{DSon} (at $V_{GS} = -4.5$ V) is 35 m Ω
- Drain current I_D is -36 A

Furthermore, the absolute maximum ratings are given in Figure 2.9 below.

ABSOLUTE MAXIMUM RATINGS ($T_C = 25$ °C, unless otherwise noted)				
PARAMETER		SYMBOL	LIMIT	UNIT
Drain-Source Voltage		V_{DS}	-60	V
Gate-Source Voltage		V_{GS}	± 20	
Continuous Drain Current	$T_C = 25$ °C	I_D	-36	A
	$T_C = 125$ °C		-21	
Continuous Source Current (Diode Conduction) ^a		I_S	-60	
Pulsed Drain Current ^b		I_{DM}	-100	
Single Pulse Avalanche Current	L = 0.1 mH	I_{AS}	-36	
Single Pulse Avalanche Energy		E_{AS}	64.8	mJ
Maximum Power Dissipation ^b	$T_C = 25$ °C	P_D	68	W
	$T_C = 125$ °C		22	
Operating Junction and Storage Temperature Range		T_J, T_{stg}	-55 to +175	°C
Soldering Recommendations (Peak Temperature) ^{d, e}			260	

Figure 2.9 Absolute Maximum Ratings of the MOSFET

2.2.1.2. Voltage Regulator

The battery voltage we are focusing on to examine further is totally modular here in this project, with a maximum of 60 V of the limit, of course. Since we cannot feed our circuit with this amount of voltage, we need to shrink it down so that we can feed our whole circuitry at the logic level.

Notably, we want a PCB that is efficiently small enough, so the discrete solutions for the voltage regulation are discarded.

There are two types of the regulator that should be considered for the project, the Linear Regulators and the Switching Regulators. Since this part of the thesis does not aim to give detailed information about the regulators, simple pros and cons comparison between the two is considered to be enough, which can be seen from Figure 2.10 below.

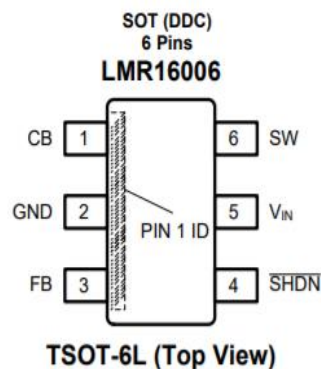
Regulator	Linear	Switching
Function	Only steps down; input voltage must be greater than output	Steps up, steps down, or inverts
Efficiency	Low to medium, but actual battery life depends on load current and battery voltage over time; high if $V_{IN} - V_{OUT}$ difference is small	High, except at very low load currents (μA), where switch-mode quiescent current (I_Q) is usually higher
Waste Heat	High, if average load and/or input/output voltage difference are high	Low, as components usually run cool for power levels below 10W
Complexity	Low, which usually requires only the regulator and low-value bypass capacitors	Medium to high, which usually requires inductor, diode, and filter caps in addition to the IC; for high-power circuits, external FETs are needed
Size	Small to medium in portable designs, but may be larger if heatsinking is needed	Larger than linear at low power, but smaller at power levels for which linear requires a heat sink
Total Cost	Low	Medium to high, largely due to external components
Ripple/Noise	Low; no ripple, low noise, better noise rejection	Medium to high, due to ripple at switching rate

Figure 2. 10 Comparison between Linear and Switching Regulators [17]

Because of its efficiency and the reduced area compared to the linear regulators, a Chopper-Buck converter regulator is adapted to the BATMAN project. Of course, it will have more noises, but since we do not have any component that would cause to have significantly high transient currents, this would be a better solution for the system.

The LMR16006 is a PWM DC/DC buck regulator, which is, of course of a step-down type. With a broad input scope of 4 V to 60 V, it is appropriate for a broad scope of use from mechanical to auto for power molding from an unregulated source. In ECO mode, Buck's standby current is around 28 μ A, which is appropriate for battery working frameworks. An ultra-low 1 μ A closure current can additionally sustain the battery life. [18]

The simplified schematic and the pinout of LMR16006XDDCR is given below in Figure 2.11 below.



Pin Functions

PIN		I/O	DESCRIPTION
NAME	NUMBER		
CB	1	I	Switch FET gate bias voltage. Connect C_{boot} cap between CB and SW.
GND	2	G	Ground connection.
FB	3	I	Feedback Input. Set feedback voltage divider ratio with $V_{OUT} = V_{FB} (1+(R1/R2))$.
SHDN	4	I	Enable and disable input (high voltage tolerant). Internal pull-up current source. Pull below 1.25 V to disable. Float to enable. Establish input undervoltage lockout with two resistor divider.
V_{IN}	5	I	Power input voltage pin. Input for internal supply and drain node input for internal high-side MOSFET.
SW	6	O	Switch node. Connect to inductor, diode, and C_{boot} cap.

Figure 2. 11 LMR16006XDDCR pinout [18]

The LMR16006 is advanced for up to 600 mA load flows. It has a typical 0.765 V feedback voltage. The gadget has implicit security highlights, for example, beat by the current beat cutoff, temperature detecting, and closure because of unnecessary power consumption. [18]

The absolute maximum ratings of the LMR16006XDDCR is given in Figure 2.13 below.

		MIN	MAX	UNIT
Input Voltages	V _{IN} to GND	-0.3	65	V
	SHDN to GND	-0.3	65	
	FB to GND	-0.3	7	
	CB to SW	-0.3	7	
Output Voltages	SW to GND	-0.3	65	
	SW to GND less than 30 ns transients	-2	65	
T _J Operation Junction temperature		-40	150	°C

Figure 2. 12 Absolute maximum ratings of LMR16006XDDCR [18]

Apart from selecting the component, the surrounding needed circuit elements are also very important. The example of a typical LMR16006XDDCR application circuit, for 5V output, in this case, can be seen from Figure 2.14 below.

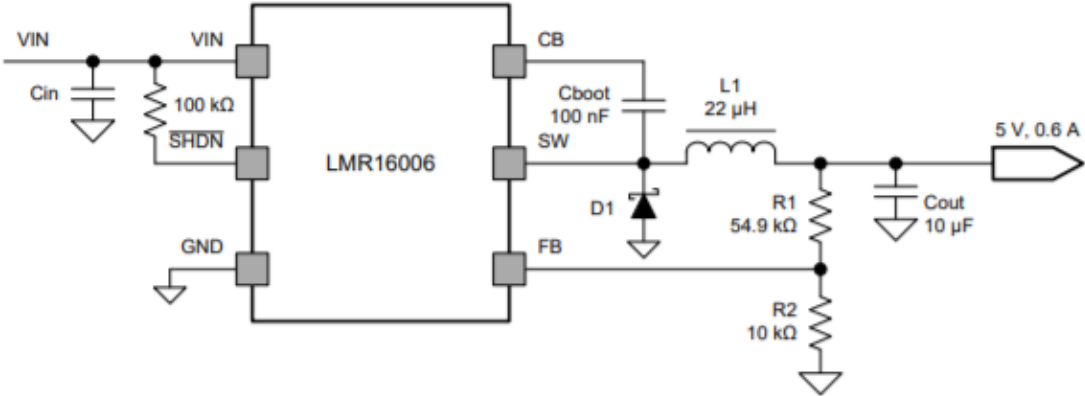


Figure 2. 13 Example application circuit of LMR16006XDDCR [18]

This Buck converter is a PWM DC-DC step-down converter. It does not need a feedback resistor configuration as in the figure above because the LMR16006XDDCR already has an internal voltage divider that will provide a fixed $3.3\text{ V} \pm 3\%$ output.

However, the other elements of the application should be carefully selected, as explained below in detail.

- **Input Capacitor**

C_{in} , the input capacitor, is a bulk capacitor. It avoids large voltage transients that may occur at the input of the converter as a result of switching. The main idea is that the C_{in} should have a ripple current that is greater than the maximum input current ripple, which can be calculated with Formula 2.5 below.

$$I_{in,ripple} = I_{out} \frac{V_{out}}{V_{in,min}} \frac{(V_{in,min} - V_{out})}{V_{in,min}} \quad (2.5)$$

Furthermore, the maximum input ripple voltage can be calculated by using the input capacitance C_{in} , which should be chosen between $0.1\ \mu\text{F}$ and $10\ \mu\text{F}$. The higher the value of the input capacitance, the lower the input ripple voltage will be due to the inverse proportion.

$$V_{in,ripple} = \frac{0.25 I_{out,max}}{f_{sw} C_{in}} \quad (2.6)$$

- **Bootstrap Capacitor**

The reason why we need the Bootstrap capacitor, C_{BOOT} , is that we need a charge pump operation. The C_{BOOT} value should be chosen between $0.1\ \mu\text{F}$ and $1\ \mu\text{F}$, which depends on the difference between the input and the output voltages.

Since, for this project, the input voltage is considerably higher than the output voltage of the Buck converter, it is better to choose the lowest value for the C_{BOOT} .

- **Output Inductor**

There are two main parameters when calculating the output inductance that is the peak current and the DC resistance.

The output inductance is connected to the ripple current, the input, and the output voltages of the peak-to-peak inductor. The maximum input voltage, since the ripple current rises with the input voltage, is often used to calculate the inductance. The minimum value of the output inductor can be calculated using Formula 2.7 below.

$$L_{out,min} = \frac{(V_{in,max} - V_{out})}{I_{out} K_{IND}} \frac{V_{out}}{V_{in,max} f_{sw}} \quad (2.7)$$

The KIND coefficient reflects, relative to the maximum output current, the sum of inductor ripple current. So the formula becomes;

$$I_{ripple} = \frac{(V_{in,max} - V_{out}) V_{out}}{L_{out} V_{in,max} f_{sw}} \quad (2.8)$$

Finally, we need to know the RMS current and saturation current ratings for the output filter inductor so that we do not exceed them. They can be calculated from the below formulas.

$$I_{L-RMS} = \sqrt{I_{out}^2 + \frac{1}{12} I_{ripple}^2} \quad (2.9)$$

$$I_{L-peak} = I_{out} + \frac{I_{ripple}}{2} \quad (2.10)$$

- **Output Capacitor**

The importance of the selection of the output capacitance is highly effective on both the output voltage ripple and the regulator's response to a hefty load current change.

We can calculate the minimum output capacitance with the below Formula 2.11.

$$C_{out} > \frac{2\Delta I_{out}}{f_{sw}\Delta V_{out}} \quad (2.11)$$

While the load current decreases rapidly, an output voltage overshoot will be generated by the stored energy in the inductor. So, when switching from a high load current to a lower load current, the output capacitor must also be sized to absorb the energy contained in the inductor. The formula below is used to measure the minimum capacitance to hold the overshoot of the output voltage at the desired value.

$$C_{out} > L_{out} \frac{(I_{oh}^2 - I_{ol}^2)}{(V_f^2 - V_i^2)} \quad (2.12)$$

In addition, in order to satisfy the output voltage ripple requirements, we can calculate the required minimum output capacitance.

$$C_{out} > \frac{1}{8f_{sw}} \frac{1}{\frac{V_{o_ripple}}{I_{L_ripple}}} \quad (2.13)$$

Finally, the formula below calculates the maximum ESR (equivalent series resistance) for the output capacitor to have in order to satisfy the output voltage ripple specifications.

$$R_{ESR} < \frac{V_{o_ripple}}{I_{L_ripple}} \quad (2.14)$$

2.2.1.3. Current and Voltage Sensing

The aim of this project, as mentioned many times before, is to calculate the SoC and SoH of the concerning connected battery by using some parameters. Those parameters for this specific project are basically voltage and current. By using the voltage and the current together, we will be able to provide an accurate SoC and SoH of the battery.

So in order to get the voltage and the current, we need a sensing circuitry in order to provide a correct value for both of the parameters.

For the voltage measuring, the idea is simple. What is needed to be done is simply to measure the voltage of the source.

For the current measuring, as mentioned before, with the reasons, a shunt resistor will be used, of which value is very small in order not to affect the correct system behavior by introducing comparably big voltage potential drops.

There are many ways in order to acquire these parameter values and send them to the microcontroller in order for them to be utilized to get an accurate SoC and SoH. For our case, it would be better to think of the different ways as two separate approaches.

The first one is to use a distinct external integrated circuit component that is totally able to get both the voltage and the current and, using its inner ADC (Analog to Digital Converter), converts them to digital information so that it can send that data to the microcontroller.

There are many different sense amplifiers for that purpose. Table 2.1 shows a quick comparison between the possible sense amplifiers.

PARAMETERS	INA226-Q1	INA225-Q1	INA220-Q1	LMP860x-Q1
Shunt V measurement	Yes	Yes	Yes	Yes
Bus V Measurement	Yes	No	Yes	No
Output Type	I2C	Analog	I2C	Analog
Resolution	16	-	12	-
Shunt Accuracy	$\pm 0.02\%$	$\pm 0.1\%$	$\pm 0.2\%$	$\pm 0.2\%$
Bus Accuracy	$\pm 0.02\%$	-	$\pm 0.2\%$	-
Alert function	Yes	No	No	No
CMRR	126 dB	95 dB	120 dB	90 dB
Bandwidth	3.5 kHz	200 kHz	5.5 kHz	60 kHz
Gain	1	200 100 50 25	1 0.5 0.25 0.125	100 50 20
Programmable gain	No	Yes	Yes	No
Gain Error	0.1	0.15	0.5	0.5
Offset Voltage	$10\mu V$	$150\mu V$	$50\mu V$	$1000\mu V$

Table 2. 3 Comparison Among different sense amplifiers [11]

However, for this project, it would be wise to choose the digital ones over the analog ones since it will be more efficient and more straightforward to utilize the I²C communication protocol, which is supported both in the sense amplifier and the microcontroller.

Considering a better resolution and CMRR (common-mode rejection ratio) and also a lower offset, INA226-Q1 seems to be the best choice for our purpose.

One may worry about its small bandwidth. However, it should also be noted that the current variations in a car battery system are comparably slow. It may even further be thought of as an advantage, as we know that with higher frequencies, the components are nothing but noise. [11]

The INA226-Q1 is a current shunt and power screening with an interface that is viable with the I2C communication protocol. The gadget just screens both a shunt voltage drop and bus supply voltage. The way that it likewise has programmable calibration esteem, transformation times, and averaging, joined with an inside multiplier, empowers some immediate readouts of current in amperes and power in watts. [19]

The pinout of the INA226-Q1 can be seen in Figure 2.15 below.

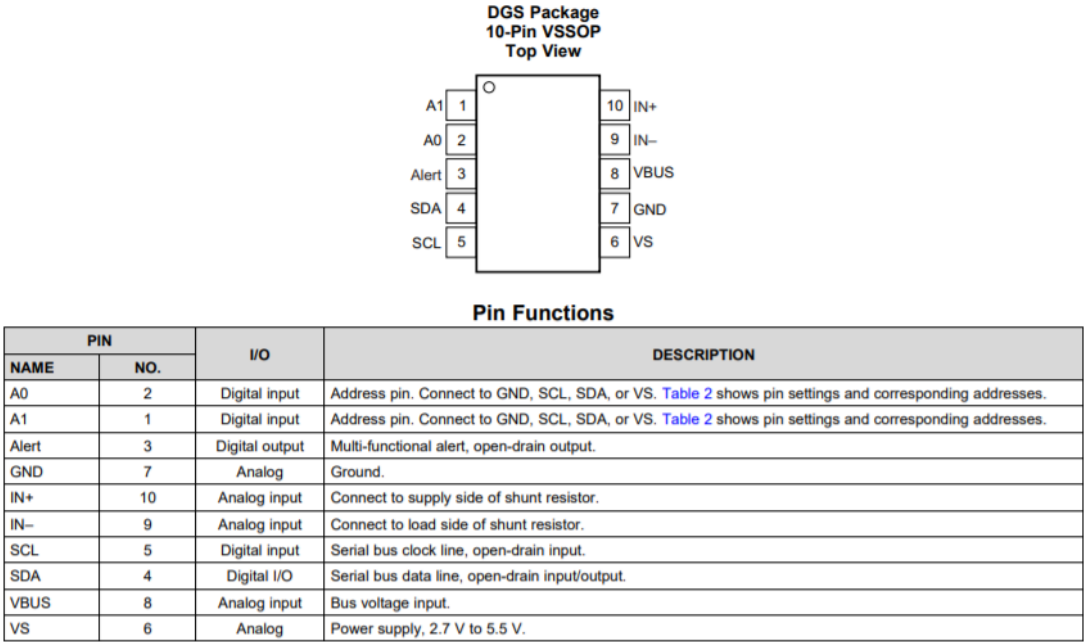


Figure 2. 14 INA226-Q1 pinouts [19]

For additional data on the gadget specifications, the INA226-Q1 applies current detecting on the bus voltages that can differ from 0 V to 36 V, free of the supply voltage. The gadget works from a solitary 2.7 V to 5.5 V stockpile, and it draws around 330 μA of supply current. The gadget is determined over the operating temperature range between – 40°C and 125°C, and it likewise includes up to 16 programmable address locations on the I 2C-viable interface. [19]

Even though it seems like a fine choice for our system, it has its own drawbacks and disadvantages also. Since it is very expensive to have such a sophisticated integrated circuit component in the PCB, and also it causes a lot of area consumption, it is decided that it would be wiser to use the ADC of the microcontroller itself.

That means, for acquiring the voltage and current value, a conditioning circuitry will be needed before sending the analog data to the microcontroller pins.

For this purpose, simple operational amplifiers will be used for both voltage and current measurements. The whole sensing circuitry is given in Figure 2.15 below.

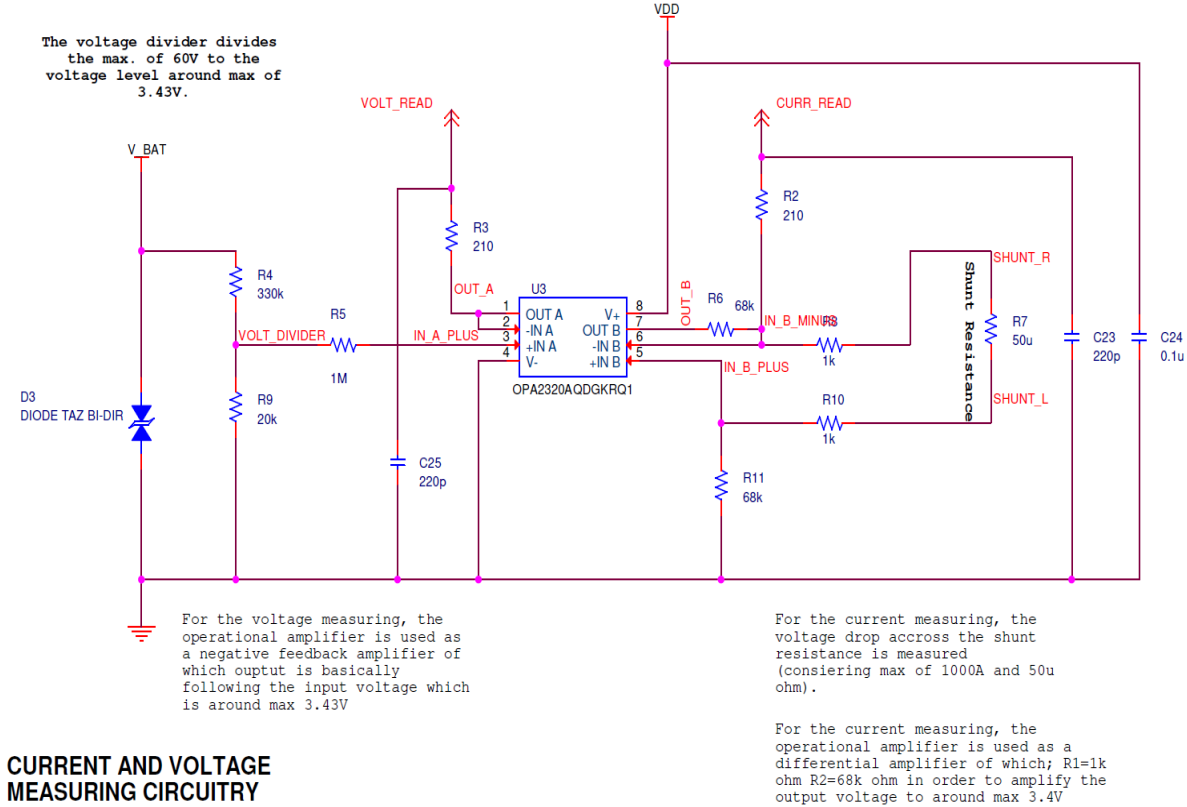


Figure 2. 15 Current and Voltage Measuring Circuitry

For the voltage measuring, the operational amplifier is used as a negative feedback amplifier, of which output is basically following the input voltage, which is around max 3.43V.

Of course, before sending the analog voltage value to the negative feedback amplifier, it needs to be lowered to the logic levels. For this purpose, a simple voltage divider is used, of which calculations are done according to the following formulas.

$$V_{Divided} = V_{BAT} \frac{R_1}{R_1+R_2} \quad (2.15)$$

Considering a maximum V_{BAT} voltage of 60 V, and the corresponding resistors with 20 k Ω and 330 k Ω , the formula becomes as follows.

$$V_{Divided,max} = 60V \frac{20 \text{ k}\Omega}{20 \text{ k}\Omega+330 \text{ k}\Omega} \quad (2.16)$$

$$V_{Divided,max} = \sim 3.43 \text{ V} \quad (2.17)$$

That means the maximum logic voltage that will be supplied to the negative feedback operational amplifier is 3.43 V, which is acceptable for the logic level pins.

A negative feedback amplifier is an electronic amplifier that deducts from its info a negligible portion of its yield such that the first signal is limited by negative input. [20] The negative feedback applied will boost its presentation (gain power, linearity, frequency reaction, phase response) and, due to assembly or setting, decrease the affectability of boundary varieties. On account of these preferences, numerous amplifiers and control frameworks utilize negative feedback. [21]

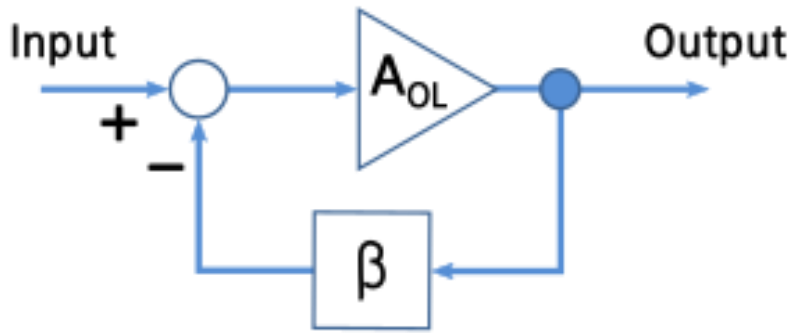


Figure 2. 16 Ideal negative-feedback amplifier

Where A_{OL} is the amplifier gain, β is the feedback network by which the output signal is acquired and transforms in some way, such as attenuation or filtering.

The following formulas give the idea about the working principle of the negative feedback amplifier.

$$V_{out} = A_{OL}V'_{in} \quad (2.18)$$

Suppose that βV_{out} is applied as a fraction of the output to one of the inputs by an attenuating feedback loop such that it subtracts from the V_{in} the input voltage of the circuit applied to the other input. The subtraction result applied to the input of the amplifier is as follows.

$$V'_{in} = V_{in} - \beta V_{out} \quad (2.19)$$

We can substitute V'_{in} in the Formula 2.18 to get the below expression.

$$V_{out} = A_{OL}(V_{in} - \beta V_{out}) \quad (2.20)$$

$$V_{out}(1 + \beta A_{OL}) = V_{in}A_{OL} \quad (2.21)$$

Finally, the gain of the amplifier with feedback called the closed-loop gain A_{FB} becomes as follows.

$$A_{FB} = \frac{V_{out}}{V_{in}} = \frac{A_{OL}}{1 + \beta A_{OL}} \quad (2.22)$$

Here is the pros and cons information of the negative feedback amplifiers.

Pros [22]

- The input and output impedance can be increased or decreased
- It offers a wide bandwidth
- It reduces total distortion if applied enough.
- It desensitizes the gain of the amplifier to variations in components.
- It can regulate the phase response of the amplifier.

Cons [22]

- In order to prevent instability, careful design attention is required.
- A negative feedback amplifier's input and output impedances become sensitive to the gain of an amplifier without feedback, which brings changes in the open-loop gain across these impedances.
- It alters the distortion composition (increasing audibility) if applied insufficiently.

For the current measuring, as mentioned before, a shunt resistor will be used. This shunt resistor will have a very low resistance value ($\sim 50 \mu\Omega$) so that the correct behavior of the system is not affected by a significantly high voltage drop on it.

On the two terminals of the shunt resistor, a differential amplifier will be used in order to measure the voltage difference between the two terminals and then amplify it to a logic value in order to be able to apply it to the microcontroller.

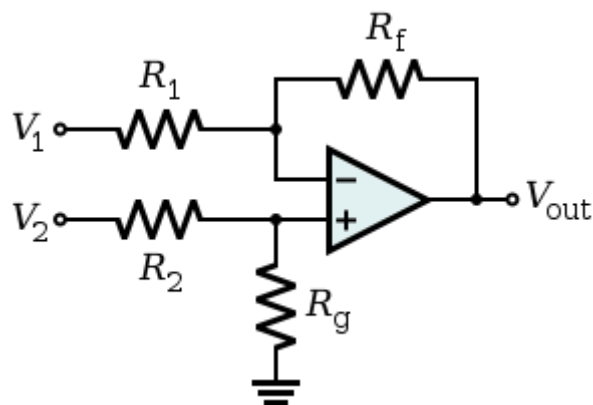


Figure 2. 17 Op-amp differential amplifier

In order to understand the working principle of this differential amplifier, the following formulas will be introduced.

$$V_{out} = \frac{(R_f + R_1)R_g}{(R_g + R_2)R_1} V_2 - \frac{R_f}{R_1} V_1 \quad (2.23)$$

For most of the cases, in order to have the maximum efficiency and for the sake of simplicity, we can consider $R_1 = R_2$ and $R_f = R_g$, and the formula becomes as follows.

$$V_{out} = \frac{R_f}{R_1} (V_2 - V_1) \quad (2.24)$$

Here is the pros and cons information of the differential amplifiers.

Pros [23]

- They allow us to have a good noise cancellation
- They can significantly reduce the external interference
- They are linear
- In order not to have unwanted signal, they increase the CMRR

Cons [23]

- They can be complex in terms of circuitry
- In order to utilize them efficiently, proper biasing may be needed

2.2.1.4. Shunt Resistor

When selecting a shunt resistor, some criteria should be considered. Two of the most important ones are the resistance and the power rating. As mentioned many times before in this thesis, the resistance value should be very small in order not to have a significant voltage drop across the terminals of the shunt resistor because we want the system to be adequately fed with a proper voltage.

In Table 2.1, we have seen that the maximum current to be 985 A. In order to compensate for the possible failures due to higher current effects, we can approximate this value to 1000 A, also for simplicity.

Since we have chosen to use a differential amplifier for the conditioning circuitry, the shunt voltage range is extensive and flexible, which is between **-0.5 V** and **+0.5 V**. So, starting from that estimation, we can calculate the maximum power rating and hence the optimal resistance value for the shunt resistor.

$$R_{Shunt} < \frac{V_{max}}{I_{max}} = \frac{0.5 V}{1000A} = 500 \mu\Omega \quad (2.25)$$

Then use this value as a maximum R_{Shunt} value, we can calculate P_{max} .

$$P_{max} = R_{Shunt} I_{max}^2 = 500 \mu\Omega \cdot (1000 A)^2 = 500 W \quad (2.26)$$

This implies that the maximum power dissipated on the shunt resistor should be 500 W at maximum. Since this power value is significantly high, it will be easier to choose the resistance for the shunt resistor.

We should consider the available commercial values for the resistance, and it would be wise to use a resistance value that will cause a comparably lower power dissipation. For example, **50 $\mu\Omega$** would be a good choice for the shunt resistor as it will approximately dissipate **50 W**, which is totally tolerable for the system.

In Figure 2.18 below, the shunt resistor is depicted.



Figure 2. 18 WSBM8518 Resistor with its Package and Molex Connector [24]

For further information, the detailed features of the shunt resistor are given below. [24]

- The power to resistor size ratio is very high
- Proprietary processing technique produces extremely low resistance values
- It has a resistive element with a low TCR ($< 20 \text{ ppm}/^\circ\text{C}$)
- The PCB connection is easy due to the molded enclosure
- Includes 4-pin male connector that mates with a Molex type MX150 #33472-4001 female connector
- The inductance of the resistor is very low ($< 5 \text{ nH}$)
- It has a low thermal EMF ($< 1 \mu\text{V}/^\circ\text{C}$)

2.2.1.5. Temperature Sensors

We know that temperature has an effect on both the components and the calculations, which cannot be negligible.

One of the reasons why we need a temperature measurement is that we need to compensate for the thermal drifts of the components due to the temperature changes. This is because when dealing with systems like ours, the thermal drift due to the temperature changes cannot be neglected. Especially if the system has a protection circuit composed of protective diodes, due to the fact that the diode's forwarding bias voltage drop affects the measured supply voltage, thermal drifts are very effective.

The other important reason for having a temperature measurement is that when calculating SoC and SoH, apart from the parameters voltage and current, there is one more parameter, which is temperature. So we have to take into account the temperature effect when calculating the desired features of the battery.

The first measurement is basically a board temperature measurement. It will be accomplished by basically soldering a temperature sensor onto the PCB itself, with its thermal pad being on the bottom of the sensor itself.

The second measurement can be called a hood temperature measurement. However, this sensor will not be hard soldered onto the PCB; instead, it will be connected onto the system case having the thermal pad facing towards the environment, namely the hood.

For these two types of measurements, the TMP112A temperature measurement sensor can be chosen, which is pretty viable for these kinds of applications.



Figure 2. 19 TMP112x family Digital Temperature Sensor

For further detailed information about the TMP112A temperature sensor, the absolute maximum ratings and the electrical characteristics are given below.

		MIN	MAX	UNIT
Supply voltage	V+		4	V
Voltage at SCL, ADD0, and SDA		-0.5	4	V
Voltage at ALERT		-0.5	((V+) + 0.3) and ≤ 4	V
Operating temperature		-55	150	°C
Junction temperature, T _J			150	°C
Storage temperature, T _{stg}		-60	150	°C

Figure 2. 20 Absolute maximum ratings of TMP112A

PARAMETER		TEST CONDITIONS	MIN	TYP	MAX	UNIT
TEMPERATURE INPUT						
Temperature range			-40		+125	°C
Accuracy (temperature error)	TMP112A	+25°C, V+ = 3.3 V		±0.1	±0.5	°C
		0°C to +65°C, V+ = 3.3 V		±0.25	±0.5	
		-40°C to +125°C		±0.5	±1	
	TMP112B	+25°C, V+ = 1.8 V		±0.1	±0.5	
		0°C to +65°C, V+ = 1.8 V		±0.25	±0.5	
		-40°C to +125°C		±0.5	±1	
TMP112N	-40°C to +125°C			±1		
DC power-supply sensitivity		-40°C to +125°C		0.0625	±0.25	°C/V
Long-term drift ⁽¹⁾		3000 hours at 125°C		±0.0625		°C
Resolution (LSB)				0.0625		°C
DIGITAL INPUT/OUTPUT						
Input capacitance				3		pF
V _{IH}	Input logic level		0.7 (V+)		3.6	V
V _{IL}			-0.5		0.3 (V+)	
I _{IN}	Input current	0 < V _{IN} < 3.6 V			1	μA
V _{OL SDA}	Output logic level	V+ > 2 V, I _{OL} = 3 mA	0		0.4	V
		V+ < 2 V, I _{OL} = 3 mA	0		0.2 (V+)	
V _{OL ALERT}	Output logic level	V+ > 2 V, I _{OL} = 3 mA	0		0.4	V
		V+ < 2 V, I _{OL} = 3 mA	0		0.2 (V+)	
Resolution				12		Bits
Conversion time				26	35	ms
Conversion modes		CR1 = 0, CR0 = 0		0.25		Conv/s
		CR1 = 0, CR0 = 1		1		
		CR1 = 1, CR0 = 0 (default)		4		
		CR1 = 1, CR0 = 1		8		
Timeout time				30	40	ms
POWER SUPPLY						
Operating supply range			+1.4		+3.6	V
I _Q	Average quiescent current	Serial bus inactive, CR1 = 1, CR0 = 0 (default)		7	10	μA
		Serial bus active, SCL frequency = 400 kHz		15		
		Serial bus active, SCL frequency = 3.4 MHz		85		
I _{SD}	Shutdown current	Serial bus inactive		0.5	1	μA
		Serial bus active, SCL frequency = 400 kHz		10		
		Serial bus active, SCL frequency = 3.4 MHz		80		

Figure 2. 21 Electrical characteristics of TMP112A

2.2.1.6. Microcontroller

The microcontroller is the heart and brain of the system. It should be chosen with great attention in order for the system to work correctly with the above mentioned external circuitries and the peripherals.

We need to set some requirements so that a good choice can be made. The primary needs are listed below.

The microcontroller should;

- be able to acquire the analog values correctly
- have an ADC with enough resolution and accuracy
- communicate with the temperature sensors via I²C protocol
- evaluate the SoC and SoH with the given parameters
- send and receive data via BLE by communicating with an app

In the light of the above-mentioned criteria, the CC2640R2F-Q1 microcontroller from Texas Instruments seems like a wise choice as it will fulfill all the requirements with excellent efficiency.

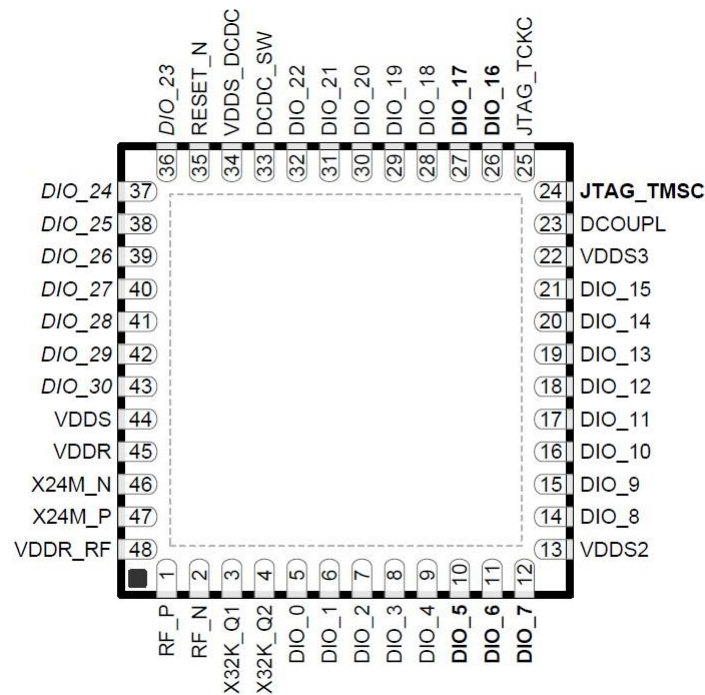


Figure 2. 22 CC2640R2F-Q1 pinout

The main specifications of the CC2640R2F-Q1 are listed below. [25]

- Efficient Arm ® Cortex ®-M3
- The clock speed of up to 48-MHz
- 275-KB non-volatile memory, including 128-KB Programmable Flash in-system memory
- Temperature level 2 of the device:-40 ° C to +105 ° C atmospheric working temperature range
- 31 GPIOs can be routed to any GPIO with all-digital peripheral pins.
- ADC 12-bit, 200-samples/s, 8-channel MUX analog
- Wide voltage range of supply: 1.8 to 3.8 V
- Using I²C Protocol
- Temperature sensor which is embedded inside
- 2.4-GHz Bluetooth low energy (BLE) 4.2 and 5 specifications compliant RF transceiver
- Link budget of 102 dB for Low Energy Bluetooth 1 Mbps

Finally, for a quick glance to observe the working principle of the CC2640R2F-Q1, a detailed functional block diagram is depicted below.

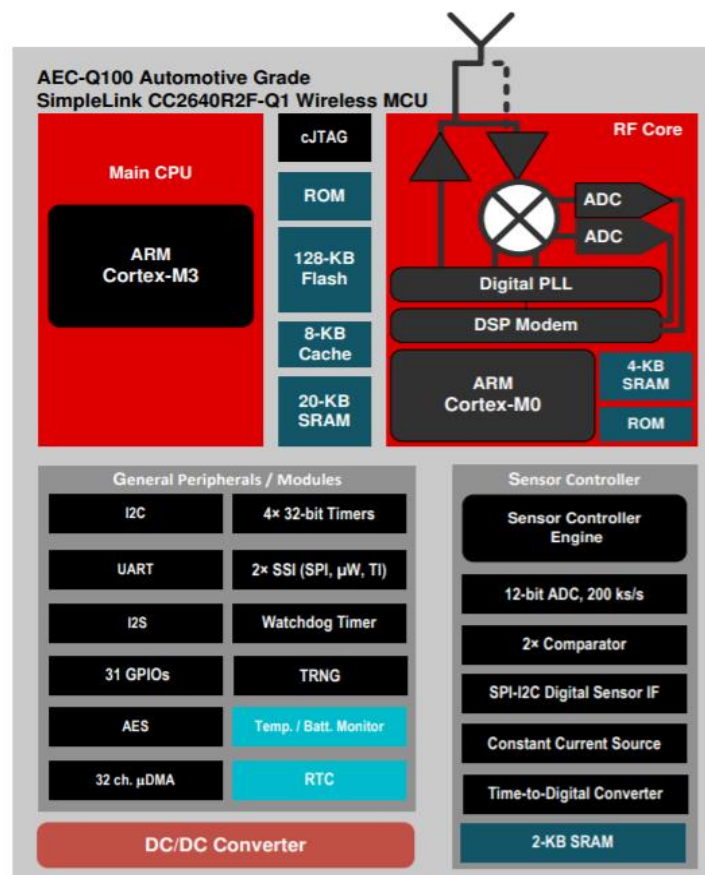


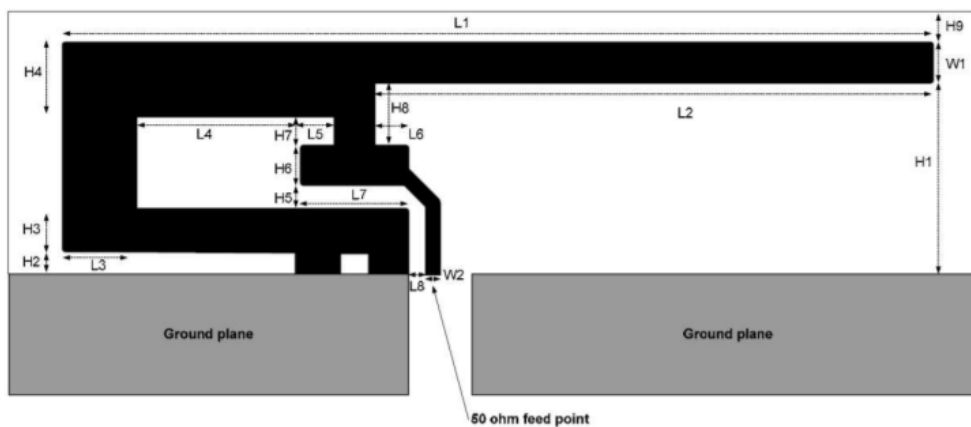
Figure 2. 23 CC2640R2F-Q1 functional block diagram [25]

2.2.1.7. Antenna

For the antenna selection, there are basically two solutions. Either a PCB trace antenna or a ceramic chip antenna will be used.

The reason why a trace antenna on a PCB should be considered is that it provides a method of wireless communication, and during the PCB manufacturing, the trace is laminated specifically on the PCB surface. Also, in some cases, the traces can be placed as several layers of a multilayer board, in which cases the PCB vias are used in order to interconnect the traces on each layer. Feeding the antenna is typically arranged with a microstrip line that is simply the trace lines of the PCB.

For an example look of a possible implementation, the DN007 from Texas Instruments layout is depicted in the following figure along with the related dimensions.



H1	5.70 mm	W2	0.46 mm
H2	0.74 mm	L1	25.58 mm
H3	1.29 mm	L2	16.40 mm
H4	2.21 mm	L3	2.18 mm
H5	0.66 mm	L4	4.80 mm
H6	1.21 mm	L5	1.00 mm
H7	0.80 mm	L6	1.00 mm
H8	1.80 mm	L7	3.20 mm
H9	0.61 mm	L8	0.45 mm
W1	1.21 mm		

DN007 layout and dimensions [26]

Here is the pros and cons comparison for the trace antenna solution.

Pros

- Since the trace is applied as a part of the PCB assembly process, the manufacturing costs are relatively low
- It has an extremely simple structure and, because
- The structured profile is very thin since the antenna is on the PCB
- It has a very large bandwidth

Cons

- It is not very cost-effective as they consume a lot of areas
- Objects are too close to the antenna area on the PCB
- During the operation, they become in contact with people, which is bad
- The tuning of the antenna should be adjusted each time the PCB layout is changed since the antenna performance and tuning are highly affected by the PCB design

Notably, a detailed antenna matching analysis has been studied from the Master Thesis named “Current and Voltage Sensing Circuit for Automotive Batteries SoH and SoC Determination” of Federico Di Fazio and Davide Fazi from Politecnico di Torino written in 2019. [11]

However, there could occur a massive problem if the previously mentioned patch antenna is used on the PCB. The fact that a shunt resistor is going to be used for the circuit, its case strictly limits the dimensions and the sizes of the PCB. For that reason, it will not be a wise choice to use a trace patch antenna. That leads us to consider the other option, which is the ceramic antenna.

Here is a pros and cons comparison of the ceramic antennas.

Pros

- They are external and distinct components that can be thought of as separate
- They come in small size and also with a variety of configurations
- The possibility of being close to the other components does not affect the system as much as the trace antenna solution
- Since they are ceramics, they are less affected by environmental factors or human operators when compared to the trace antennas
- They offer a variety of testing solutions and also a flexible
- Since they are distinct components, it is very easy to change them as we like

Cons

- The cost of the ceramic antenna is comparably higher than trace solutions
- In order to optimize the ceramic antenna, a good level of RF expertise may be needed

A 2.4 GHz mini ceramic antenna can be selected from Johanson Technology.



Figure 2. 24 2450AT18A100E 2.4 GHz Mini Antenna

For further detailed information, the general specifications and the mechanical dimensions are given in the following figures.

General Specifications	
Part Number	2450AT18A100
Frequency (MHz)	2400 - 2500
Avg. Rad Efficiency*	76%
Peak Gain (dBi typ.)	0.5
Average Gain (dBi typ.)	-0.5
Return Loss (dB)	9.5 min.
Impedance	50 Ω
Input Power	2 Watts max. (CW)

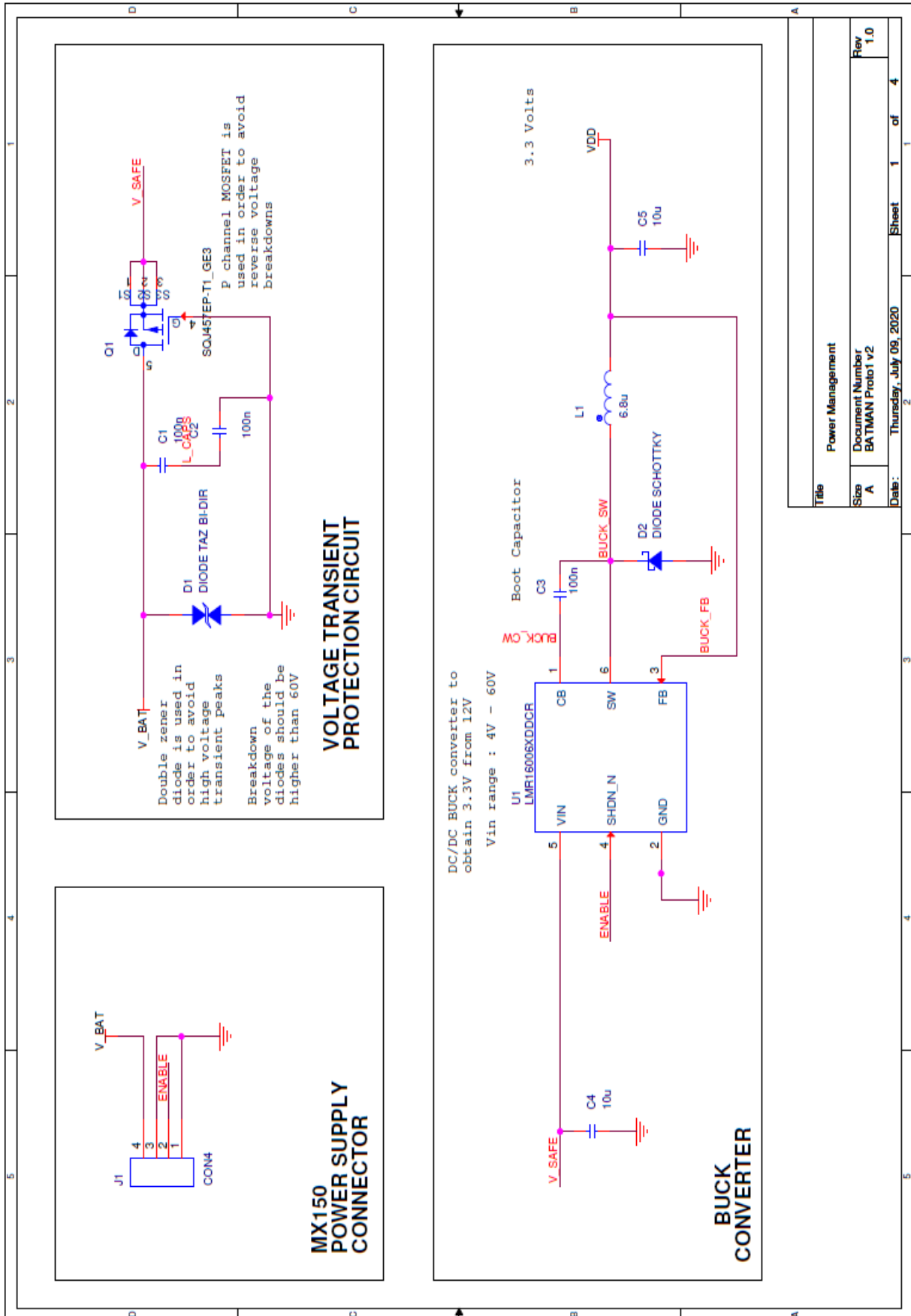
Figure 2. 25 2450AT18A100 antenna general specs [27]

Mechanical Dimensions		
	In	mm
L	0.126 \pm 0.008	3.20 \pm 0.2
W	0.063 \pm 0.008	1.60 \pm 0.2
T	0.051 +.004/-0.008	1.30 +0.1/-0.2
a	0.020 \pm 0.012	0.50 \pm 0.3

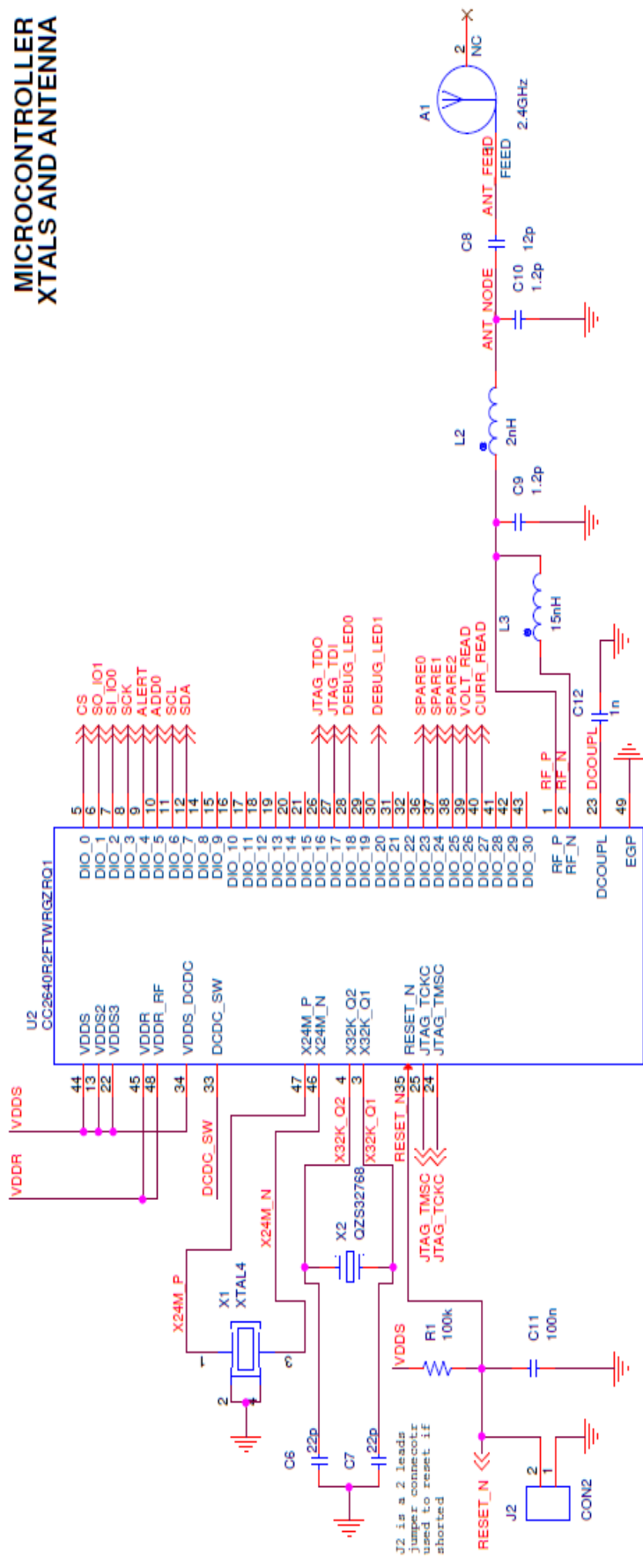
The figure shows two views of the antenna. The top view is a rectangle with length L and width W, containing a smaller brown square in the center. The side view shows a horizontal cylinder with a small rectangular protrusion on its right side. The width of this protrusion is labeled 'a' and its height is labeled 'T'.

Figure 2. 26 2450AT18A100 mechanical dimensions [27]

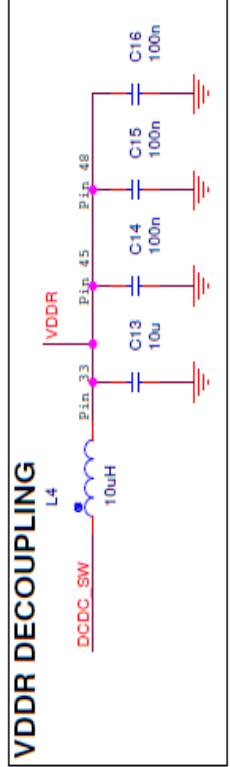
2.2.2. Schematic Explanation



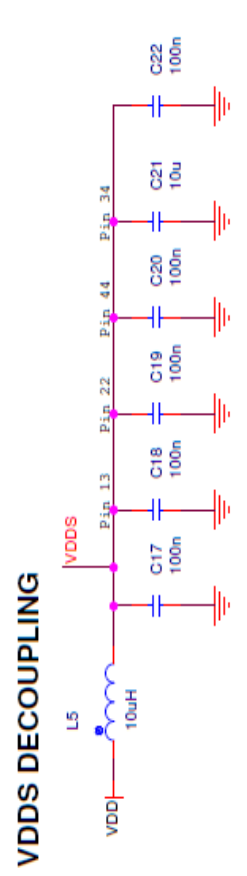
MICROCONTROLLER XTALS AND ANTENNA



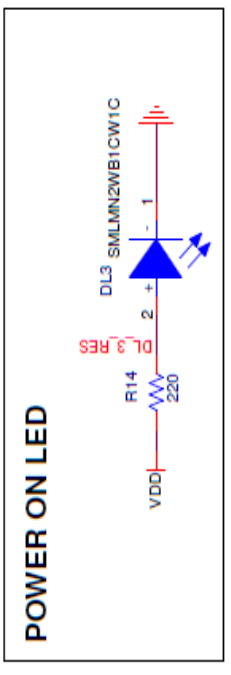
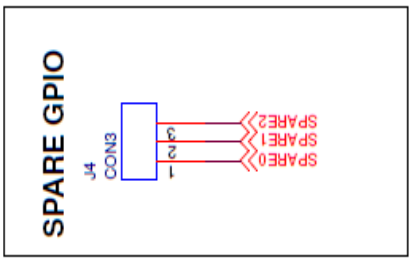
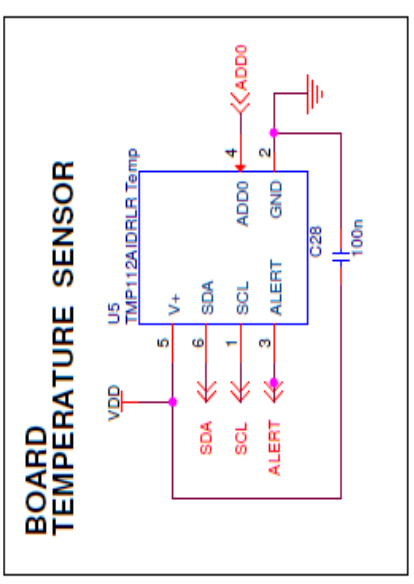
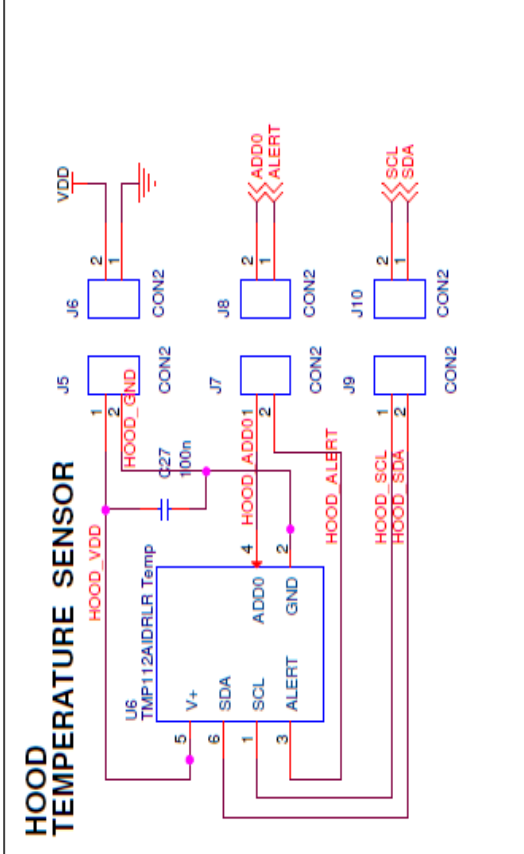
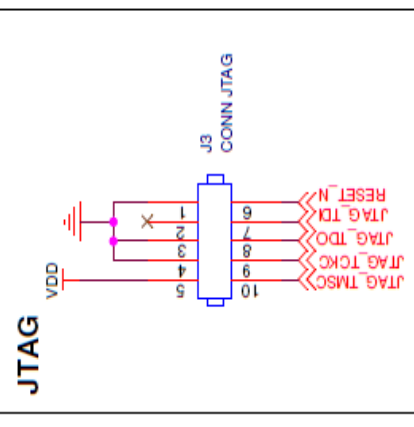
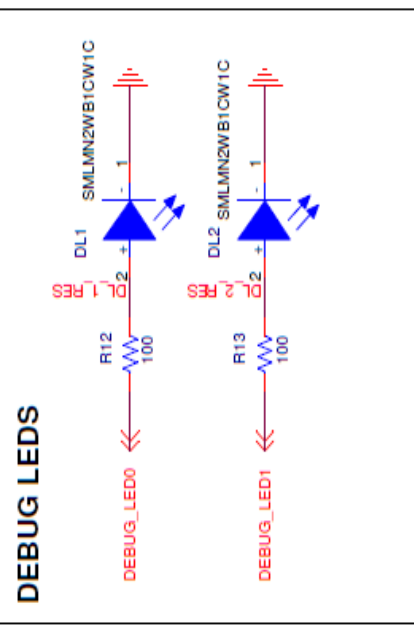
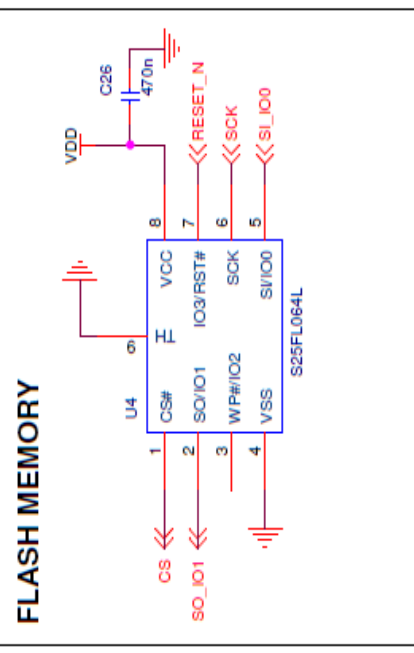
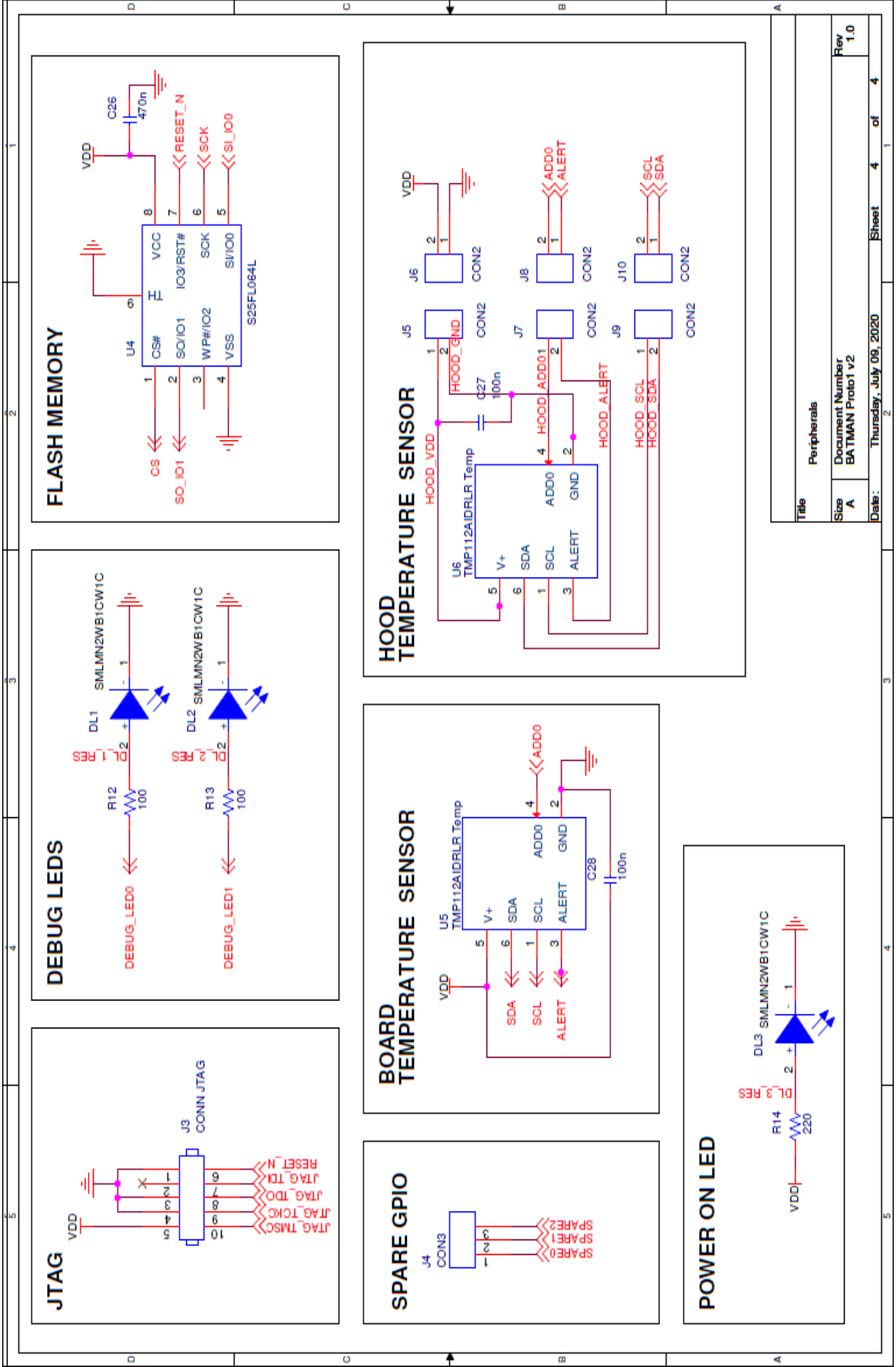
VDDR DECOUPLING



VDD5 DECOUPLING



Title	Microcontroller
Size	A
Document Number	BATMAN Proto1 V2
Date:	Thursday, July 09, 2020
Sheet	2 of 4
Rev	1.0



Title		Peripherals	
Size	A	Document Number	BATMAN Proto1 v2
Date:	Thursday, July 09, 2020	Sheet	4 of 4
Rev	1.0		

2.2.2.1. Voltage Transient Protection Circuit

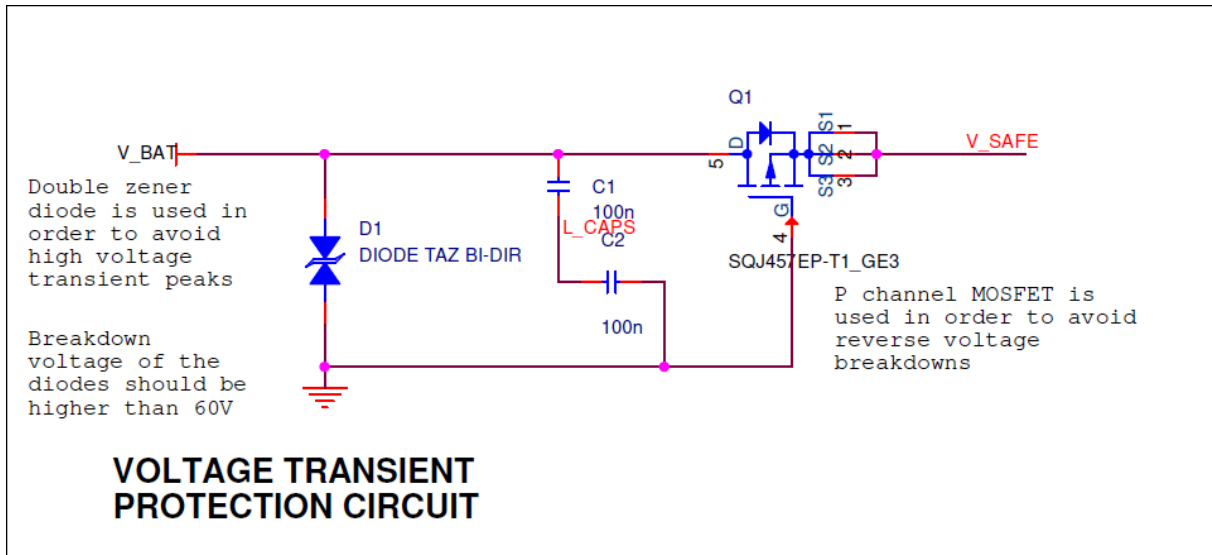


Figure 2. 27 Voltage Transient Protection Circuit

A detailed explanation of the voltage transient protection has been done in subsection 2.2.1.1.

For a piece of quick information, the writings in Figure 2.27 can be seen as they have some information on the fundamental reasons why the protective circuit elements are placed and used.

2.2.2.3. Microcontroller, XTALs, and Antenna

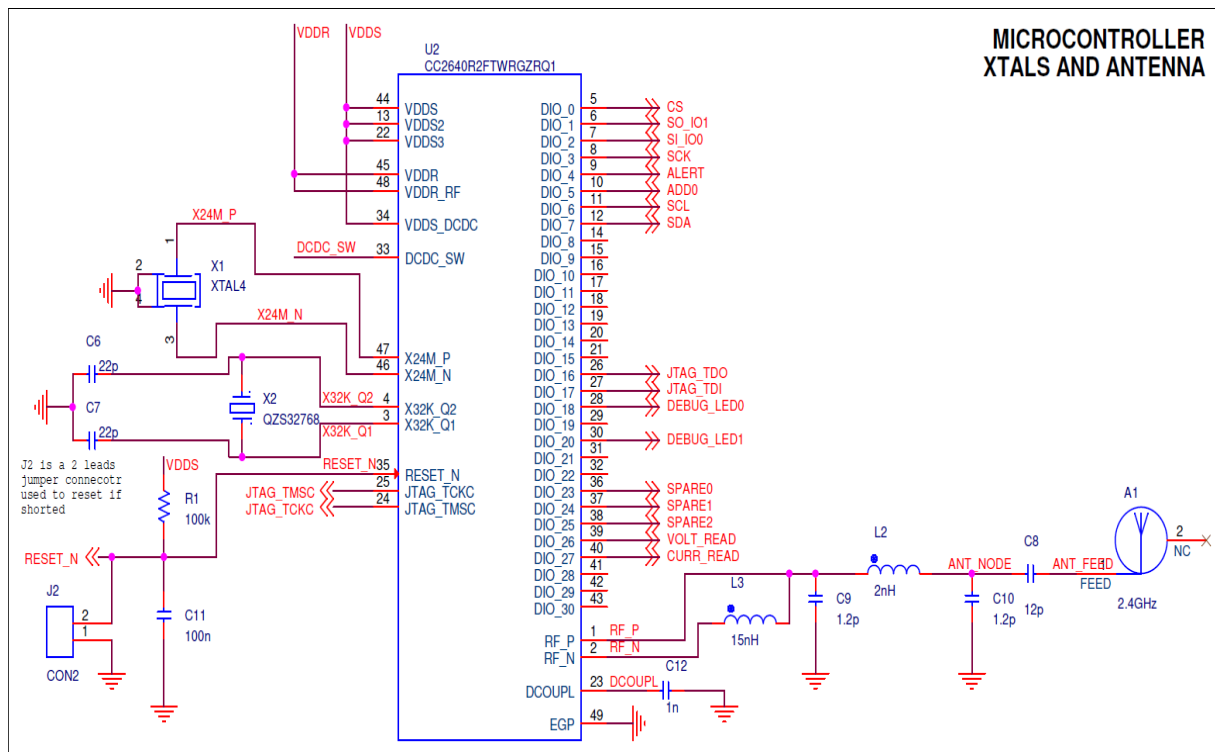


Figure 2. 29 Microcontroller, XTALs, and Antenna

- **CON2:** An active-low reset connector
- **R1, C11:** The passive components of the active low reset
- **C12:** Decoupling capacitor
- **L3:** Balun inductance
- **L2, C9, C10:** The passive elements of the LC filter
- **C8:** The matching capacitor
- **X1:** The 24MHz XTAL needed to make the microcontroller's main clock
- **X2:** The 32.768kHz XTAL needed to make a precise low-frequency oscillator

2.2.2.4. Decoupling

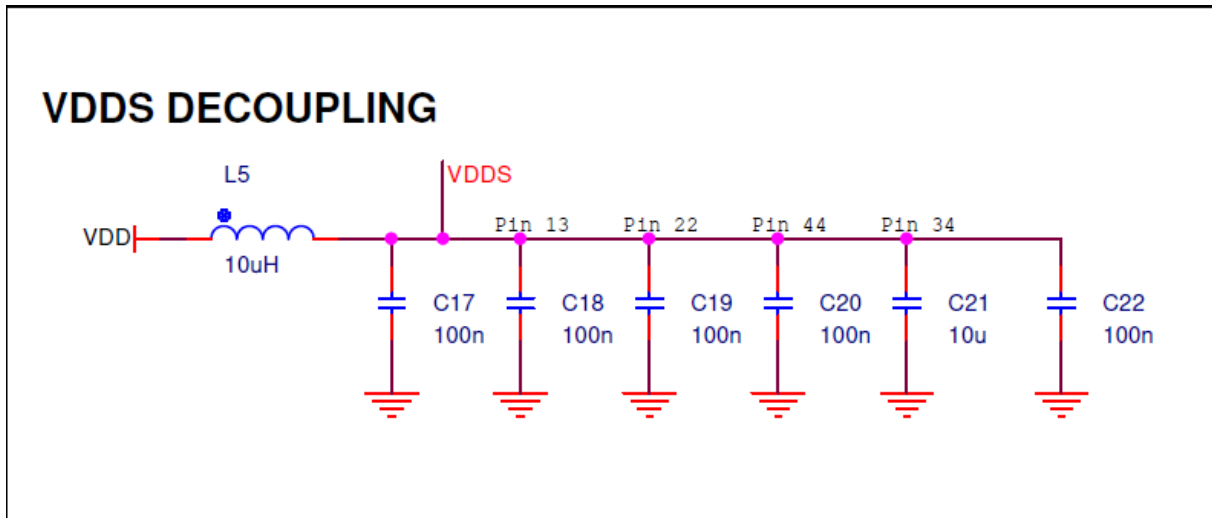


Figure 2. 30 VDDS Decoupling

- **C17:** Protective capacitor against possible EMC problems
- **C18:** Decoupling capacitor
- **C19:** Decoupling capacitor
- **C20:** Decoupling capacitor
- **C21:** Decoupling capacitor
- **C22:** Decoupling capacitor
- **L5:** Ferrite core inductance for EMC compliance

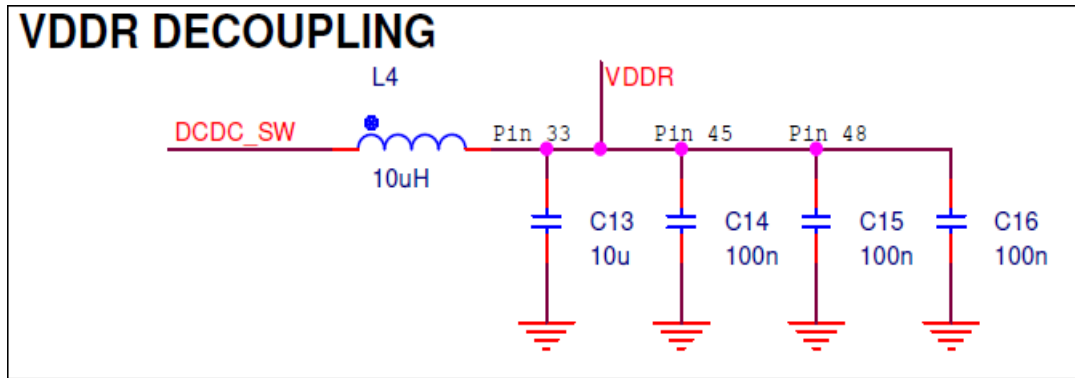


Figure 2. 31 VDDR Decoupling

- **L4:** External inductance needed for the internal DCDC switching
- **C13:** External capacitance needed for the internal DCDC switching voltage regulator
- **C14:** Decoupling capacitor
- **C15:** Decoupling capacitor
- **C16:** Protective capacitor against possible EMC problems

2.2.2.5. Current and Voltage Measuring Circuitry

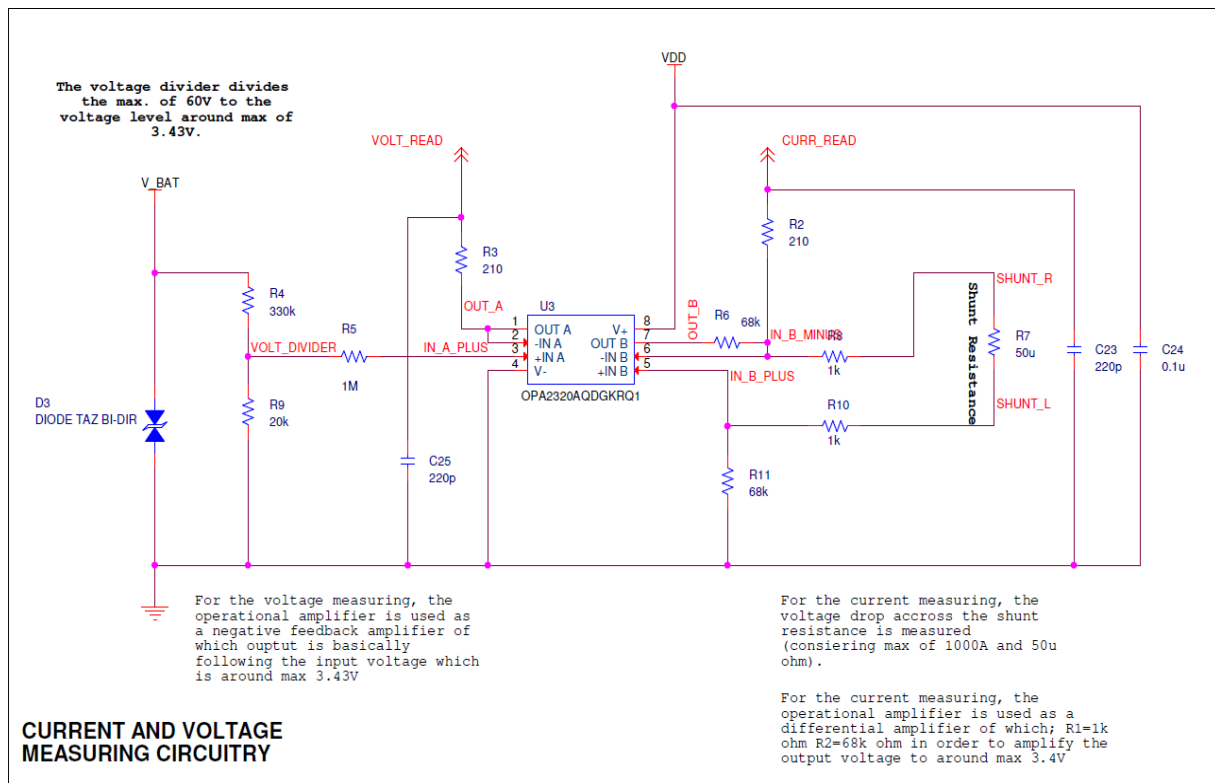


Figure 2. 32 Current and Voltage Measuring Circuitry

- **D3:** Transient voltage protection diode
- **R4 and R9:** Voltage divider resistors
- **R5:** Bypass resistor for voltage adjustment
- **R2 and R3:** Pull-up resistors
- **R7:** The shunt resistor
- **R6:** Differential amplifier feedback resistor
- **R8:** Differential amplifier negative input resistor
- **R10:** Differential amplifier positive input resistor
- **R11:** Differential amplifier positive input pull-down resistor
- **C23, C24, and C25:** Decoupling capacitors

2.2.2.6. Board Temperature Sensor

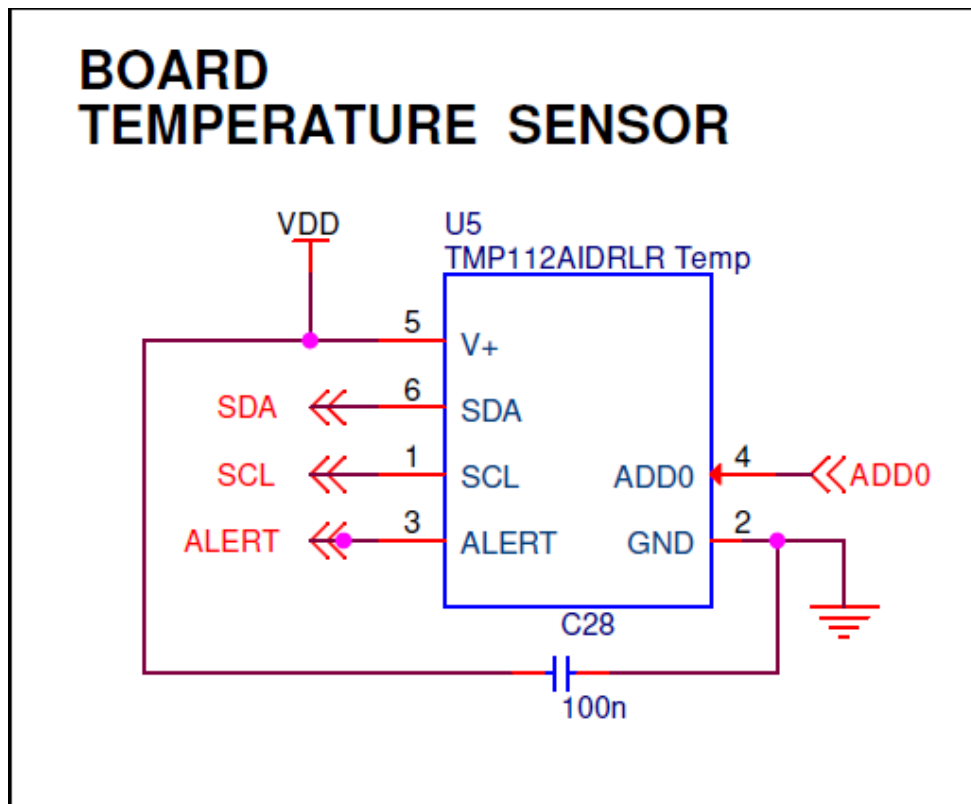


Figure 2. 33 Board Temperature Sensor

- C28: Decoupling capacitor

2.2.2.7. Hood Temperature Sensor

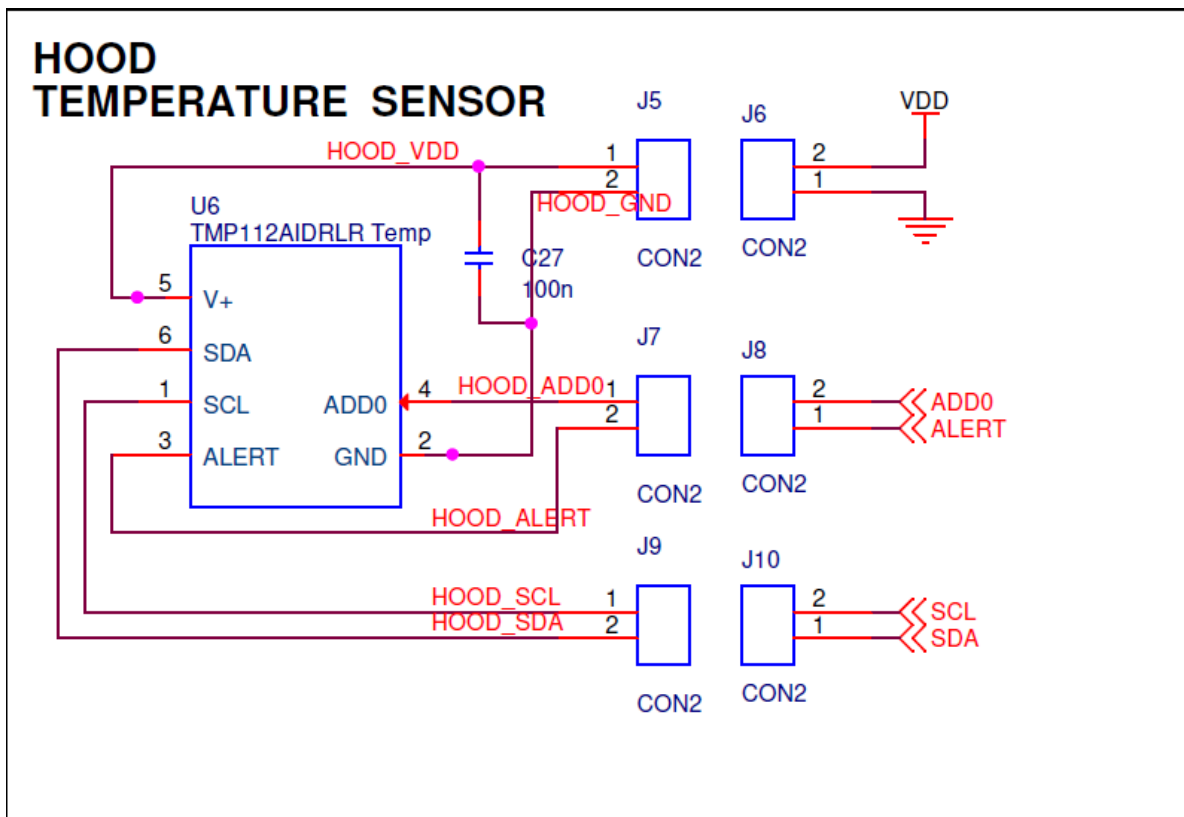


Figure 2. 34 Hood Temperature Sensor

- **C27:** Decoupling capacitor
- **J5:** The female socket soldered on TMP112A to supply the sensor
- **J6:** The male socket soldered on PCB to supply the sensor
- **J7:** The female socket soldered on TMP112A for ADD0 and ALERT pins
- **J8:** The male socket soldered on PCB for ADD0 and ALERT pins
- **J9:** The female socket soldered on TMP112A for SCL and SDA pins
- **J10:** The male socket soldered on PCB for SCL and SDA pins

2.2.3. Layout Explanation

After completing the schematic design using the *Cadence OrCAD PCB Designer* tool, the created netlist should be imported to the *Cadence Allegro PCB Designer* in order to complete the PCB design with all the components.

The resulting PCB layout is given in the figure below.

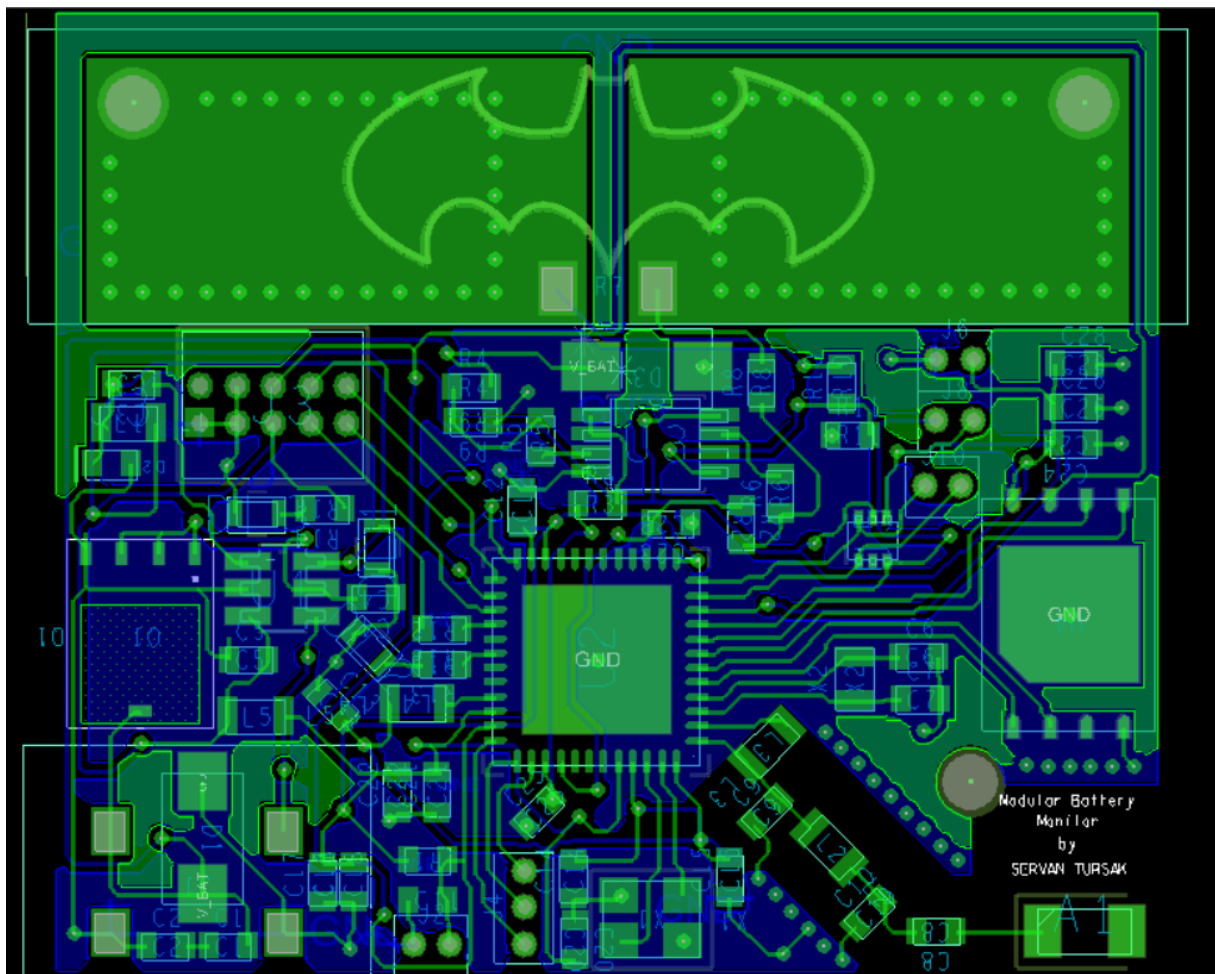


Figure 2. 35 PCB Layout

After importing the necessary netlist with all the components, they need to be placed inside the PCB carefully. There are some particular rules and key points when dealing with the component integration that are given below.

- The bypass capacitors should be placed to the related pin as close as possible and at the same time in the same layer plane
- In order to reduce the heat energy dissipated on the shunt resistor, big pads should be used
- When placing the analog and digital components together, they should be as separated as possible to avoid noises. The analog component of the project is the operational amplifier, which is used as both a negative feedback amplifier and a differential amplifier, and hence, it is placed on the upper side of the board just above the microcontroller
- The antenna always should be placed far away from the acquisition circuitry part of the board in order to avoid the noise caused by the data communication
- Also, for the same reason, the crystals that are used for clock generation should be placed far away from the acquisition part
- We know that in high frequencies, which should be highly considered for this project, the PCB traces act as individual microstrip lines. Hence, the matching circuitry of the antenna along with its components should be placed as a straight line, as seen in Figure 2.36 below, in order not to have some impedance mismatches

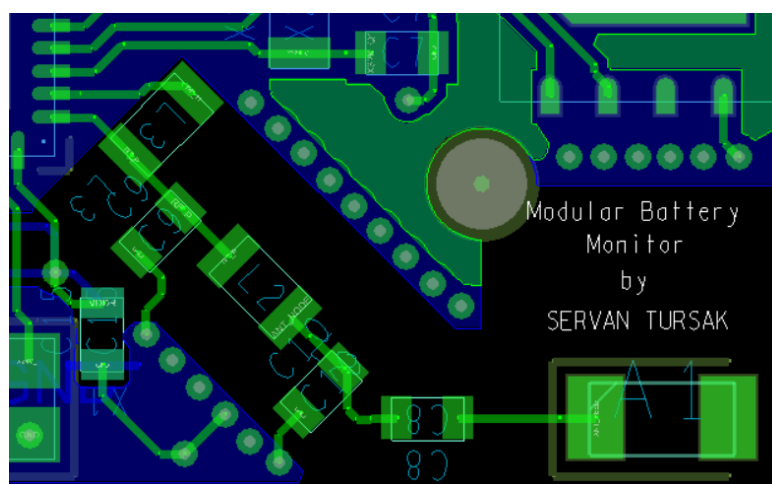


Figure 2.36 Antenna and the matching circuit components

- After physically manufacturing the PCB, one may need to replace a component in case of possible misbehavior. Because of this reason, all of the components included in the netlist should be placed on the TOP layer
- The connectors of the components should be easily accessed from the outside world

The next step after successfully placing the components is to connect each component to the other with respect to the imported netlist. Each component is connected to the other with the traces. By placing the traces, of course, a few rules should be followed, which are given below.

- If it is not strictly necessary, a long trace should be avoided, as they, in fact, introduce resistances and parasitic disturbances even though they are negligibly small
- When building a PCB, it is imperative and crucial to have the ground planes on both sides of the board. Furthermore, they need to be connected using many vias in order to ensure the equipotential state
- One should avoid having an unconnected and isolated island on the ground planes
- As an important rule, there should be no ground plane under the antenna and the matching circuit because that would cause some possible shieldings which can affect the functionality of the antenna
- Another crucial point that should be considered is that the antenna and the matching circuit should be all surrounded by the vias in order to separate that zone from the remaining board properly and also to have a proper shielding. This technique is called the *via stitching technique*, which can be seen from Figure 2.36 above.
- All the datasheets of the components should be carefully read because sometimes the manufacturer may put some useful information about the component's recommended layout

After the whole process is done, the *Gerber* files along with the *.drc* drill files should be generated and sent to the related manufacturer for physical implementation. The resulting top and bottom views can be seen from the figures below.

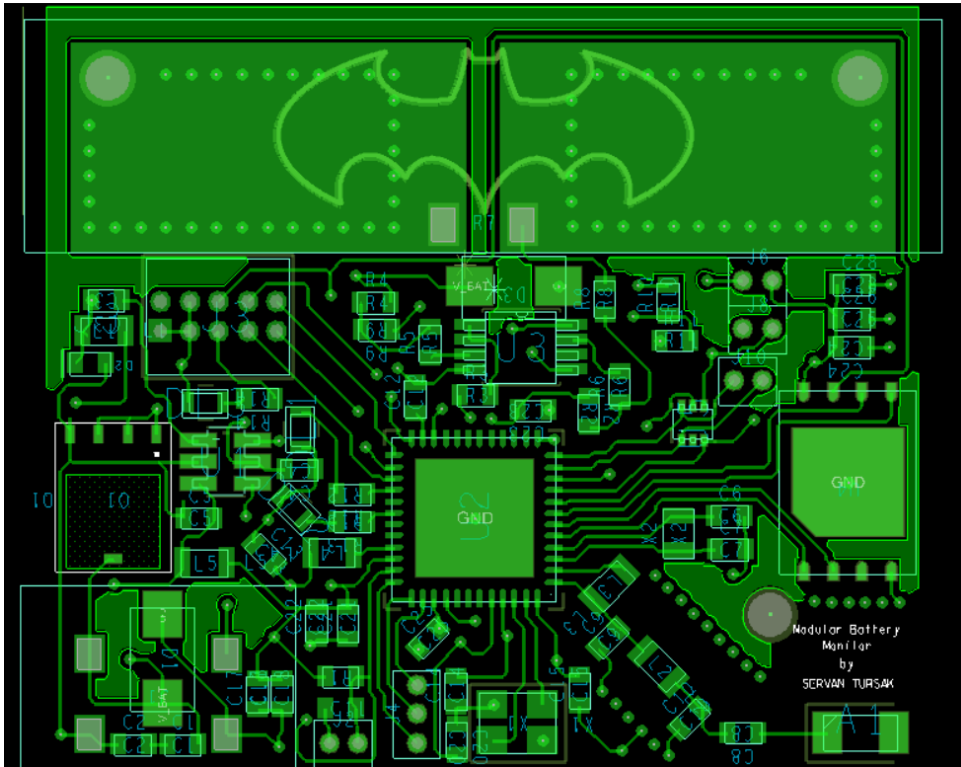


Figure 2. 37 Top View

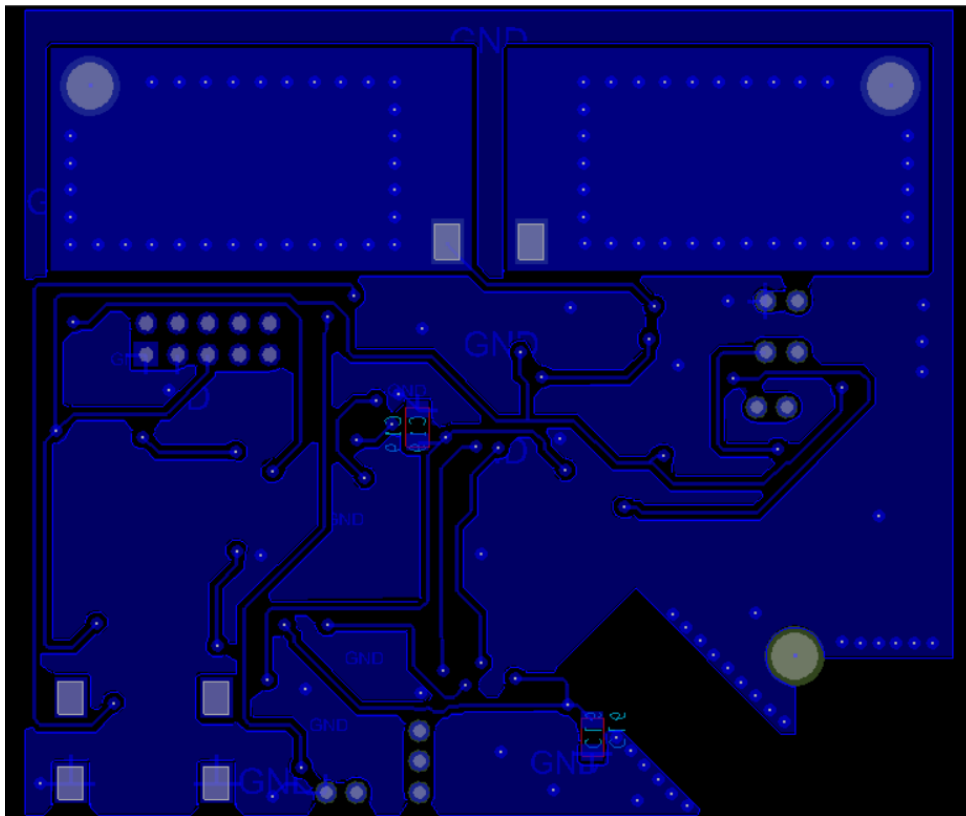


Figure 2. 38 Bottom View

2.2.4. Bill of Materials

Idx	#	Manufacturer N.	Manufacturer	Reference	Value	Unit Price
1	1	2450AT18A100E	Johanson	A1	Antenna @ 2.4GHz	0.56 €
2	15	GCM188R91E104KA37J	Murata	C1,C2,C3,C11,C14,C15,C16,C17,C18,C19,C20,C22,C24,C27,C28	100nF Capacitor	1.68 €
3	1	C0603X120J5GACAUTO	KEMET	C8	12pF Capacitor	0.34 €
4	2	D221K20Y5PL63L6R	Vishay	C23,C25	220pF Capacitor	0,356 €
5	1	C0805C102J1GAC	KEMET	C12	1nF Capacitor	0,066 €
6	2	06035A1R2K4T2A	AVX	C9,C10	1.2pF Capacitor	0.50 €
7	1	CGA3E2X5R1A105M080AA	TDK	C20	1 μ F Capacitor	0.09 €
8	2	AC0603JRNPO9BN220	Yageo	C6,C7	22pF Capacitor	0.22 €
9	1	CGA3E1X7R1C474M080AC	TDK	C26	470nF Capacitor	0.14 €
10	4	GRT188C81C106ME13D	Murata	C4,C5,C13,C21	10 μ F Capacitor	1.66 €
11	1	CDBURT0530LL-HF	Comchip Technology	D2	Schottky Diode	0.72 €
12	2	SMAJ20CAHE3/61	Vishay	D1,D3	TVS Diode	0.43 €
13	2	SML-D12U1WT86	ROHM Semiconductor	DL1,DL2	Red LED	0.19 €
14	1	SML-D12M8WT86	ROHM Semiconductor	DL3	Green LED	0.29 €
15	1	33472-4001	Molex	J1.1	RCPT Connector	2.04 €
16	4	33012-2001	Molex	J1.2	14/16AWG Connector	0.58 €
17	1	M50-1930005	Harwin	J2.1	Jumper	0.29 €
18	5	M50-3530242	Harwin	J2,J6,J8,J10	2 Pin Male	0.50 €
19	3	M50-3030242	Harwin	J5,J7,J9	2 Pin Female	1.06 €
20	1	M50-3530342	Harwin	J4	3 Pin Male	0.13 €
21	1	FTSH-105-01-L-D-K	Samtec	J3	JTAG Connector	2.79 €
22	1	KLZ2012NHR101LTD25	TDK	L1	100 μ H Inductor	0.28 €
23	1	BLM18HE152SZ1D	Murata	L5	Ferrite	0.18 €
24	1	KLZ1608MHR100WTD25	TDK	L4	10 μ H Inductor	0.23 €
25	1	MLG1005S2N0BTD25	TDK	L2	2.0nH Inductor	0.09 €
26	1	LQW18AS15NG0ZD	Murata	L3	15nH Inductor	0.22 €
27	1	SQJ457EP	Vishay	Q1	P-channel MOSFET	0.69 €
28	1	AC0603FR-07100KL	Yageo	R1	100K Ω Resistor	0.09 €
29	2	RQ73C1J210RBTFD	TE Connectivity	R2,R3	210 Ω Resistor	0.66 €
30	1	RN73R2ATTD3303B25	KOA Speer	R4	330K Ω Resistor	0.48 €
31	2	RSF100JB-73-68K	Yageo	R6,R11	68K Ω Resistor	0.1 €
32	1	WSBM8518L0500JK	Vishay	R7	50u Ω Resistor	15.26 €
33	1	TNPW08051M00BEEA	Vishay	R5	1M Ω Resistor	0.51 €
34	2	ERJ-UP3D1000V	Panasonic	R12,R13	100 Ω Resistor	0.29 €
35	2	RN73H2TD1001B10	KOA Speer	R8,R10	1k Ω Resistor	1.12 €
36	1	RC0201JR-1320KL	Yageo	R9	20k Ω Resistor	0.085 €
37	1	ERJ-UP3F2200V	Panasonic	R14	220 Ω Resistor	0.22 €
38	1	LMR16006XDDCR	Texas Instruments	U1	Buck Regulator	1.96 €
39	1	CC2640R2FTWRGZRQ1	Texas Instruments	U2	Microcontroller	7.44 €
40	1	OPA2320AQDGKRQ1	Texas Instruments	U3	Operational Amplifier	1.83 €
41	1	S25FL256LAGNFM010	Cypress Semiconductor	U4	NOR Flash	8.53 €
42	1	TMP112AIDRLR	Texas Instruments	U5,U6	TH Sensor	0.96 €
43	1	SC205-7PF20PPM	Seiko Instruments	X1	32.768kHz XTAL	0.71 €
44	1	TSX-3225 24.0000MF15X-AC3	Epson	X2	24MHz XTAL	0.32 €
Total:						57.483 €

Table 2. 4 Bill of Materials with the prices of Mouser Electronics Inc.

CHAPTER III

3. FW Implementation

3.1. RTOS

RTOS means real-time operating system, and its basic explanation would be that it is actually an operating system whose aim is to serve the real-time application processes without having the data buffers delayed since they are dealt with as they come. It has its time constraints very well defined, and hence if those constraints are not met, the whole system will fail.

The essential advantage of an RTOS is that it has a very low interrupt latency and, of course, a very low thread switching latency. However, it should be noted that, when evaluating an RTOS, the most important thing is that how fast or how accurate it can operate, not the amount of work it can perform in a given period of time.

The primary goals of an RTOS are the following.

- **Small latency:** It is real-time, so it has to be fast.
- **Determinism:** Since it's real-time, we need to know how long it takes for a particular job to be processed to ensure that no deadlines are missed.
- **Structured Software:** The software can be considered using a divide and conquer method, with which the addition of external components into the application would be more straightforward.
- **Scalability:** This should allow us to scale from a simple to a complex application with stacks, drivers, file systems, etc.
- **Offload development:** By using an RTOS, we manage more than one aspect of our system; for example, with proper scheduling, the RTOS deals with power management, interrupt table management, memory management, exception, etc.

Every RTOS has an embedded scheduler in itself, which is responsible for managing and executing the system threads. There are two types of main scheduling ways, Preemptive Scheduling, and Time-Slice Scheduling.

Since the aim of this chapter is not to go into deeper details about the schedulers, only the basic concepts will be pointed out here.

Preemptive Scheduling: It is the most widely recognized sort among the RTOS schedulers. Using a preemptive scheduling algorithm, a running thread proceeds until it either [28]

- ultimately finished the task(for example, an ISR finishes)
- a thread with a higher priority gets ready(for this situation, the higher priority thread preempts the lower priority thread)
- the string surrenders the processor while hanging tight for an asset (for example, a task calls sleep()).

Time-slice Scheduling: This kind of scheduling guarantees that for each thread, there is a given opening to be executed. Despite that, the planning of this kind is, for the most part, not appropriate for real-time applications. Strikingly, the TI-RTOS kernel upholds time-cutting scheduling for specific assignments whenever wanted. [28]

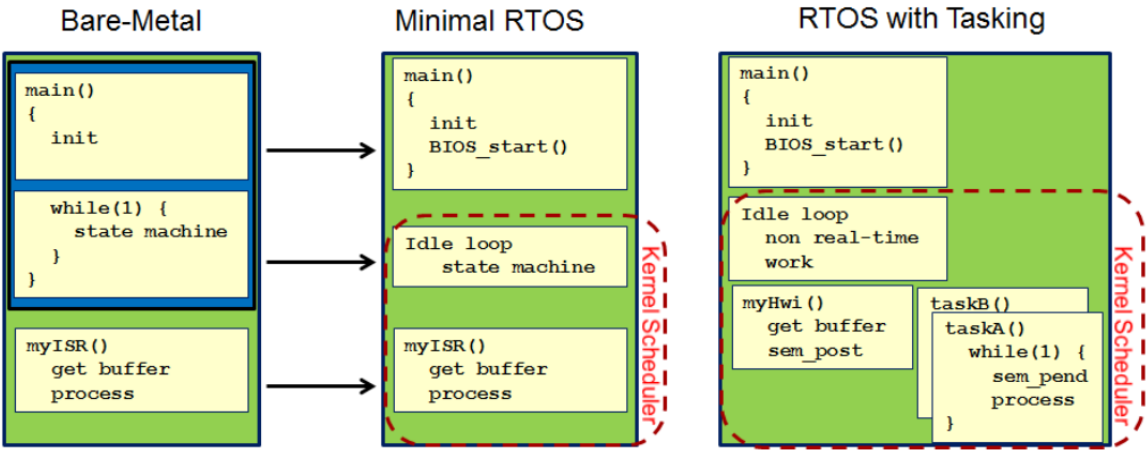


Figure 3. 1 Structure analysis from non-OS to RTOS [28]

3.2. TI-RTOS

Texas Instruments has already developed its own RTOS. It will be handy for this project since it is highly needed for BLE GATT stack operations that are the core processes of the BATMAN project.

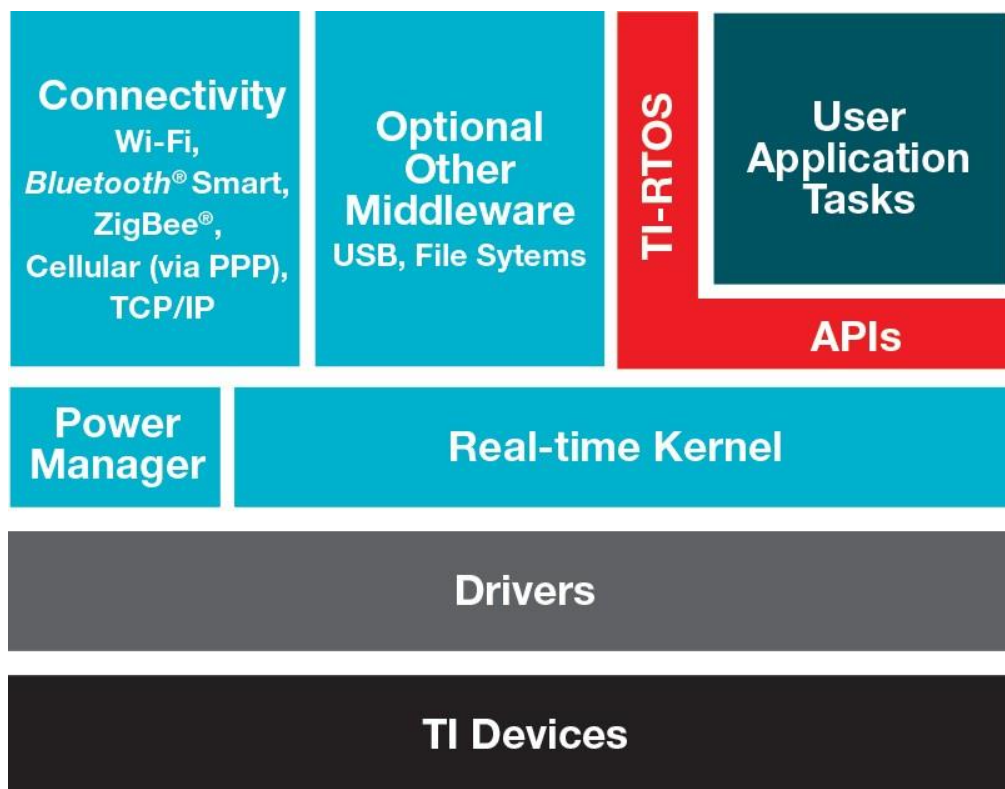


Figure 3.2 TI-RTOS Hierarchical Structure [11]

The TI-RTOS has a preemptive scheduler in its core for thread scheduling. More information regarding preemptive scheduling can be found in subsection 3.1.

3.3. Peripheral Management

The peripherals we have in this project are the temperature sensors, which are of the same type. Both of the temperature sensors, the one on the board and the external one, are responsible for measuring the board temperature and the hood temperature, respectively. Both of the sensors will communicate with the microcontroller via I²C protocol, as they compose of the related pins.

In order to utilize the I²C communication protocol of the sensors, a specific tool can be used to create the necessary piece of code to implement the proper communication protocol.

Sensor Controller (SC) is a small CPU core that allows us to manage the sensors with an interface available for both analog and digital preferences. In order to program the SC, a specific IDE called Sensor Controller Studio (SCS) can be used. For this project, specifically, the analog sensor polling task of the SCS will be used via the I²C protocol.

There is a data exchange between the Sensor Controller tasks and the System CPU application. The exchanged data is within the AUX RAM, which is shared memory. For that reason, we can create some different type definitions in order to access those variables easily by using the Sensor Controller Studio.

Notably, in order to control the SC tasks, the Sensor Controller Interface driver (SCIF) use two signals: [29]

- *To Sensor Controller:* in order to control the status of the Sensor Controller tasks the signal called "**CTRL**" is used, which starts the control operation
- *From Sensor Controller:* a signal, which represents either the interface is idle or ready to handle another task, is called **READY**

In addition, in order to have the System CPU alerted and also for exchanging data, another two signals are used by the SC: [29]

- *From Sensor Controller:* While the System CPU is in standby mode, in order to wake it up, a signal called **ALERT** is used to generate an interrupt
- *To Sensor Controller:* Also, stating that the System CPU has handled the last task and it is ready to handle another task, as an acknowledge signal, the signal **ACK** is used

There are three different pairs of C header and source files in the generated Sensor Controller Interface driver (SCIF) that needs to be put in the main application program of the project. The driver includes: [29]

- The **driver setup**:

- It has the AUX RAM image, which contains the data required by the Sensor Controller
- It includes some data structure definitions in order to handle the Sensor Controller configuration and states
- All the constant data definitions that are used in the Sensor Controller program code
- It also has information about the I/O mapping for the internal use

- An **application programming interface (API)**:

- To initialize the driver along with its I/O pin configuration
- To handle the task control of the Sensor Controller tasks
- To do the data exchange between the Sensor Controller tasks to produce input data and consume output data
- Controlling the initialization of the driver

- An **operating system abstraction layer (OSAL)**:

- It makes sure the integration with the used operating system, in our case, for example, the TI-RTOS
- It also ensures the System CPU power and clock management

As an example, here is how I²C communication is described for the temperature sensor.

Initialization

```
i2cStart();
i2cTx(DEV_ADD | I2C_OP_WRITE);
i2cTx(CONFIG);
i2cTx(cfg.config >>8);
i2cTx(cfg.config & 0xFF);
i2cStop();
fwDelayUs(15000,FW_DELAY_RANGE_100_MS); // delay of 15ms
```

Execution

```
if (state.i2cStatus == 0) {
/* ----SENDING COMMAND TO READ TEMPERATURE CONSEQUENTLY----*/

    i2cStart();
    i2cTx(I2C_OP_WRITE | DEV_ADD);
    i2cTx(TEMPERATURE);
    i2cRepeatedStart();
    i2cTx(I2C_OP_READ | DEV_ADD);
    i2cRxAck(output.tempHigh);
    i2cRxAck(output.tempLow);
    i2cStop();
    output.temperature = (output.tempHigh <<8) + output.tempLow;

}
else {
    i2cStop();
}

fwGenAlertInterrupt();
```

3.4. Main Program Development

As it is quite a known fact, BLE stack implementation is arduous to realize due to its high level of complexity. This makes the possibility of starting from scratch almost impossible, and this is where the project examples of Texas Instruments come very handy indeed.

Considering the basics of this project, the most useful starting point would be Project Zero, which already includes the BLE stack, which is a huge advantage. Simply, what Project Zero does is that it allows us to connect to a smartphone or another device through BLE and make the desired tasks work. Having different types of characteristics, Project Zero also allows us to control LEDs, control buttons, and have data communication between the devices. Of course, we can utilize this advantage in order to create our own BLE characteristics according to the project needs.

Since the Project Zero program is way too large to go into details here, the following subsections will just analyze simply the behaviors of the various functional blocks it has in order to provide a simple explanation of how it actually works.

3.4.1. Project Zero

ProjectZero_init():

This is the initialization procedure, which is called just before the main application task. It includes many features as follows;

- an application-specific BLE stack initialization
- the hardware setup
- notification of the power state
- application-specific BLE profile and service initialization

The initialization of the GPIO is all specified and declared in *Board.h*, where the related pins intended to be used with I2C, SPI, or simply as LEDs are defined.

ProjectZero_taskFxn():

This is the procedure where the main application task is. When the *BIOS_start* is called, TI-RTOS itself invokes this procedure, and then it calls an initialization function and waits for messages by entering an infinite loop.

In order to send messages, two ways are used. The first way is to use the BLE stack directly, and the second way is via the user code, such as Hardware Interrupt (HWI) or a callback (interrupt) function.

Notably, if we want this task to take action on some callbacks, we need to send messages to this task because some RTOS and Stack APIs are not available in the callback, and sending messages to this task is the way in order to dispatch the necessary actions.

ProjectZero_createTask():

This is simply the task creation function. The application task created by the user can be called here as an argument inside the *Task_construct* function.

For example, for the Project Zero project example, the *ProjectZero_taskFxn* is fed as an argument inside the *Task_construct* function.

user_processApplicationMessage():

In this procedure, the application messages are handled; however, the BLE stack messages are not handled here, only the application itself.

For instance, if we want a Software Interrupt (SWI) to call any of the BLE APIs, the SWI should send a related message to the application task to process in the task context.

3.4.2. Sensor Controller Interface

As mentioned before in subsection 3.3, using Sensor Controller Studio, the necessary piece of code can be created regarding the peripherals the system has, in our case, the temperature sensors. The generated code should be included in the main application program in order to have the temperature sensors work.

In order to achieve this, the generated Sensor Controller Interface drivers (SCIF) should be included inside the piece of source code called *project_zero.c*, which includes all the necessary procedures as mentioned above in subsection 3.4.1.

As a piece of further information, many of the sensor controller registers are memory-mapped, and hence, they are available for the system CPU to read from or write to it. These registers can be found in the *AUX_SCE:FETCHSTAT* and the *AUX_SCE:CPUSTAT* registers and can be easily accessed by using the *scifTaskData* structure. [11]

Before starting to call the initialization functions, the generated header file *scif.h* should be included in the program because it has all the constants and the variables SCS has defined.

After including *scif.h*, we can start the initialization of the SCIF driver, and we need to call three distinct functions below, which are fully described and defined in the *project_zero.c* source file.

```
scifOsalInit();  
scifOsalRegisterCtrlReadyCallback(scCtrlReadyCallback);  
scifOsalRegisterTaskAlertCallback(scTaskAlertCallback);
```

The callbacks *scCtrlReadyCallback* and *scTaskAlertCallback* are responsible for data transfer between the SC coprocessor and the main core.

And also, the function *scifStartRtcTicksNow* below can be used in order to wake up a Sensor Controller task with a frequency equal to *NHz* so that the task is repeated continuously every $1/N$ seconds.

```
scifStartRtcTicksNow(0x00010000 / N);
```

3.4.3. Bluetooth Management

ATT and GATT Introduction

Attribute Protocol (ATT) states that the data communication is over the air when considering the BLE (Bluetooth Low Energy). However, when we think of the overall communication from the BLE application side, we can say that the Generic Attribute Protocol (GATT) is used in order to exchange data. GATT can be considered as another layer just above the ATT.

Notably, the Bluetooth SIG defined many profiles in order for the ATT and GATT to work correctly with one another in coordination. As a brief description, a *profile* is a document describing how a GATT Service and GATT Characteristic are to be used for a specific application to work.

- **Attribute**

It is an addressable piece of data that ATT and GATT use. There are three main parts that it consists of, namely the Handle, UUID, and Value, as depicted in Figure 3.3 below, along with the length of each segment.

Handle	UUID	Value
16 bits	16 or 128 bits	1 to 512 bytes.

Figure 3.3 Attribute data structure

Notably, before sending them over the ATT, all of the UUIDs that are 32-bit long should be converted to 128-bit.

- **Handle:** It is the address of the attribute itself
- **UUID:** it is the type of the attribute
- **Value:** It is the data introduced as an array of bytes, which can be different depending on the different UUID

- **Characteristic**

A characteristic consists of many various attributes, defined above. Strictly, a characteristic must have at least the *value* attribute and the *declaration* attribute. What the declaration attribute actually does is that it comes just before the value attribute itself, and it merely defines if the value attribute can be read or written.

The hierarchy of the BLE always goes like this;

Service → *Characteristic* → *Value*

An example characteristic can be seen below with all the attribute segments reported.

Handle	UUID	Value	What
..
31	0x2803	02 :20:00 :AA:BB	Characteristic Declaration
32	0xBBAA	41:42:43	Characteristic Value
33	0x2803	02:22:00:AA:CC	Characteristic Declaration
34	0xCCAA	15	Characteristic Value

Figure 3.4 An example Characteristic in the form of two attributes

- **Service**

A service consists of many characteristics, which are described above. It actually includes each of the attributes from a specific service declaration to another service declaration.

An example of service can be seen below.

Handle	UUID	Value
30	0x2800	AA:AA
31	0x2803	02:20:00:AA:BB
32	0xBBAA	41:42:43
33	0x2803	02:22:00:DC:AC
34	0xACDC	4C:41:53:45:52

Figure 3. 5 An example service declaration

- **Profile**

One or more services add up to create a profile, and also it describes how the services can be utilized in order for a specific application to work.

Service Generation

Texas Instruments offers an easy-to-use online service generator tool, depicted in the below figure, in order to generate application-specific services for user projects.

The screenshot shows the 'Service' and 'Characteristic #0' configuration sections of the TI online service generation tool. The 'Service' section includes a 'Service name' field with the text 'camelCase is best for generati...', a 'Service UUID' field with '0xBABE (16-bit)', and radio buttons for '16-bit' (selected) and '128-bit'. The 'Characteristic #0' section includes a 'Char name' field with 'camelCase', a 'Char UUID' field with '0xBEEF', and radio buttons for '16-bit' and '128-bit' (selected). It also features two dropdown menus: 'Properties (shown in declaration)' with options 'GATT_PROP_READ', 'GATT_PROP_WRITE', 'GATT_PROP_WRITE_NO_RSF', and 'GATT_PROP_NOTIFY'; and 'Permissions (for ATT requests)' with options 'GATT_PERMIT_READ' and 'GATT_PERMIT_WRITE'. At the bottom, there is an 'Add Characteristic' button, a red 'Generate' button, and a checked checkbox labeled 'Include comments and #includes in output.'

Figure 3. 6 TI online service generation tool

Along with the service creation, we can create many different characteristics depending on the needs of our specific project. In our case, since we would like to measure the voltage, the current, and the temperature in order to calculate the accurate SoC and SoH, we will simply need to create their own characteristics in order to utilize the specific data sent over the BLE.

Properties of each characteristic define whether it should be readable or writable, or both. Of course, since we would like to read the data sent from the main core to the BLE device, we may want to enable the READ property.

Notably, it may be instrumental in also enabling the NOTIFY property for the characteristics as it will notify and wakes up the BLE device whenever new data is read through the BLE.

BLE Integration in the Program

The online service generation tool mentioned above creates two files, one source (.c) file, and one header (.h) file. They should be integrated inside the application program in order to enable all the BLE initializations and the utilization.

So, Initializing the characteristics inside the *project_zero.c* source file is simply the first thing to be done. In order to achieve that, the *SetParameter* routine should be utilized, which is defined in the specific service and characteristic source file created by the online service generator tool.

An example of a piece of code that can initialize all the needed characteristics is reported below.

```
uint8_t temp_val[10] = {0};

//Initialization of all the characteristics

myService_SetParameter(myVoltChar, myVoltChar_LEN, & temp_val);
myService_SetParameter(myCurrChar, myCurrChar_LEN, & temp_val);
myService_SetParameter(myBTempChar, myBTempChar_LEN, & temp_val);
myService_SetParameter(myHTempChar, myHTempChar_LEN, & temp_val);
```

As it can be seen above, we will need a holder variable in order to place the needed data and send it over to the BLE. the *SetParameter* routine takes three arguments, the characteristic name, the characteristic length, and the holder variable. By defining those, we have created our own characteristics inside our service, and from now on, the value we will send will be visible on the BLE device that we are sending the related data.

For example, if we would like to send the temperature data over the BLE, all we need to do is to fetch the required data from the SC, as explained in subsection 3.3, and to use the *SetParameter* routine, as seen below.

```
uint8 board_temp; //placeholder variable

//acquire the necessary data from the SC
board_temp = scifTaskData.temp112a.output.temperature;
myService_SetParameter(myBTempChar, myBTempChar_LEN, &board_temp);
```

CHAPTER IV

4. Verification of FW

4.1. CC2640R2 Launchpad

As a starting point, the developed firmware can be tested on a development kit which is called CC2640R2 Launchpad. The reason to use this launchpad is that CC2640R2 Launchpad has the exact same microcontroller embedded in it. So, the created firmware can be exposed to the microcontroller so that we can have a chance to see whether it works properly or not.

The most important feature that we can use is that CC2640R2 Launchpad has a BLE connection, which is the critical point of our project. We can basically try to send data using BLE and see if the sent data is correct or not.



Figure 4.1 TI CC2640R2 Launchpad

In order to see whether the correct data has been sent or not, we can use the Android app called *BLE Scanner*, which is one of the most common Android apps that can be utilized for various types of Bluetooth applications.

The idea should be simple as trying to send the correct voltage value that is read by the embedded ADC of the CC2640R2 Launchpad using the analog pins. In order to see what pins we may need, a pinout is shown in Figure 4.2 below.

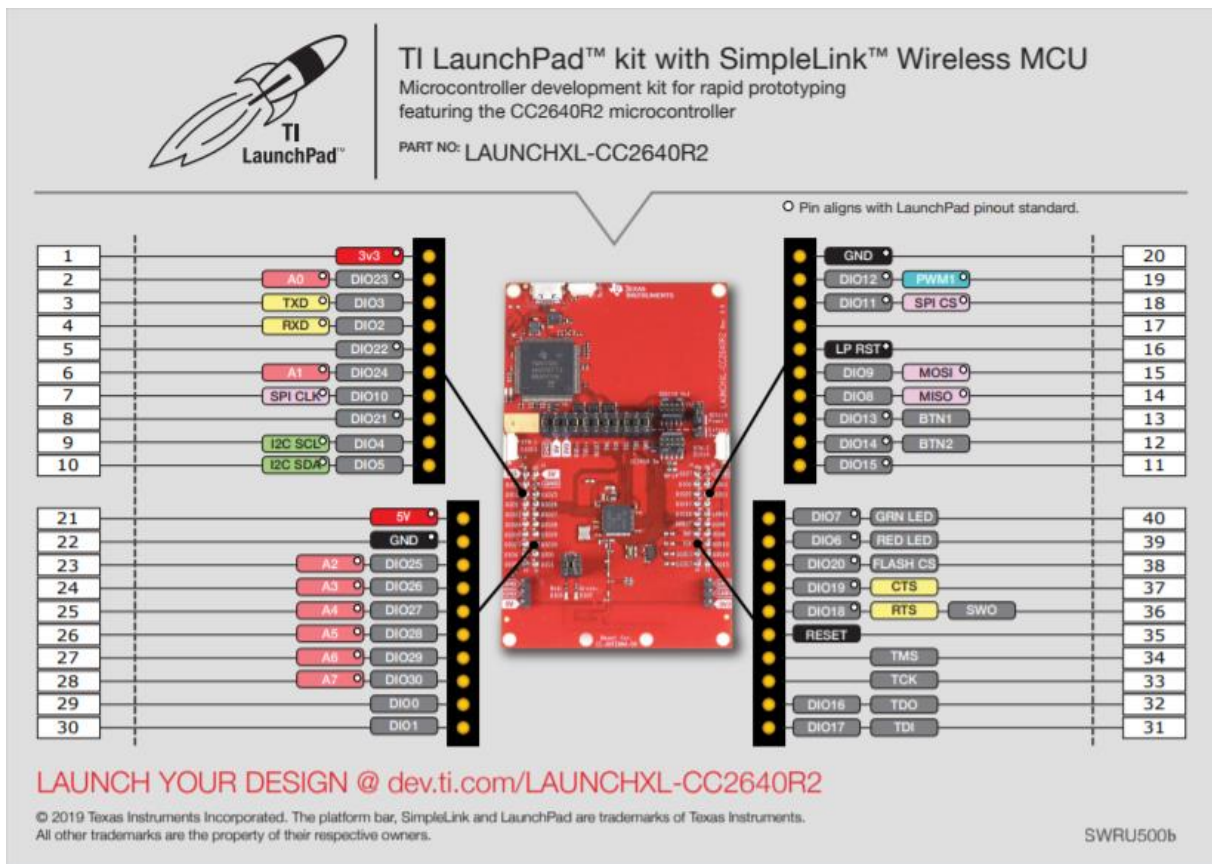


Figure 4. 2 Pinout of the CC2640R2 Launchpad [30]

For example, we can try to create some timer interrupts, and for each interrupt, we can assign some tasks for the microcontroller to do. Here is the piece of code that can be used to create timer interrupts.

```
status = timer_create(USED_CLK, &custom_sigevent, &timer_id);
if (status == -1)
    printf("ERROR Create timer");

status = timer_settime(timer_id, 0, &custom_itimerspec, 0);
if (status == -1)
    printf("ERROR Set timer");
```

After creating the timer interrupts, we can assign some periods to them so that we can utilize their full functionality. Along with the timing specifications, we should assign the other necessary parameters to create the interrupts properly.

```
custom_sigevent.sigev_notify = SIGEV_SIGNAL;
custom_sigevent.sigev_value.sival_ptr = &notifyctr;
custom_sigevent.sigev_notify_function = timerISR;
custom_sigevent.sigev_notify_attributes = NULL;

custom_itimerspec.it_value.tv_sec = nanosecs / sec_to_nsec;
custom_itimerspec.it_value.tv_nsec = nanosecs % sec_to_nsec;
custom_itimerspec.it_interval.tv_sec = nanosecs / sec_to_nsec;
custom_itimerspec.it_interval.tv_nsec = nanosecs % sec_to_nsec;
```

The above piece of code simply describes the whole parameters in order to create the necessary timer interrupt. By adjusting and changing the *nanosecs* variable, we can assign some periods to the interrupts.

Then the next step should be creating and implementing an ADC in order to read the voltage values sensed by one of the analog pins of the CC2640R2 Launchpad. The piece of code given below initiates the ADC and implements it correctly so that we can acquire the voltage value through the analog pin.

```

/* Call driver init functions */
ADC_init();

ADC_Handle  adc;
ADC_Params  params;
int_fast16_t res;

//first adc starts

ADC_Params_init(&params);
adc = ADC_open(Board_ADC0, &params);

if (adc == NULL) {
    printf("Error initializing ADC0\n");
    while (1);
}

/* Blocking mode conversion */
res = ADC_convert(adc, &adcValue0);

if (res == ADC_STATUS_SUCCESS) {
    adcValue0MicroVolt = ADC_convertRawToMicroVolts(adc, adcValue0);

    //printf("ADC0 raw result: %d\n", adcValue0);
    //printf("ADC0 convert result: %d uV\n", adcValue0MicroVolt);
    data1 = adcValue0MicroVolt;
    data1 = data1 / 1000000;
    //printf("data = %f\n", data);
}
else {
    printf("ADC0 convert failed\n");
}

```

Now that we have both the timer interrupts and the ADC implemented correctly, we can send the ADC data in whatever period we like. However, the last step for this is, of course, to implement the BLE stack for this specific application.

Since the BLE implementation is deeply covered in subsection 3.4.3, they will not be covered here again as the steps to implement the BLE for this example is pretty straightforward.

To sum up, we have created a user-specific service, and we have created the necessary characteristic for the voltage read, as explained in subsection 3.4.3.

All that needs to be done at this point is to call the *SetParameter* function and feed it with the correct variables so that we can read the value we are sending to the BLE Scanner app.

Once we build and upload the firmware in the BLE Scanner app, we can see the created service with a UUID of 0xBABE, as shown below.

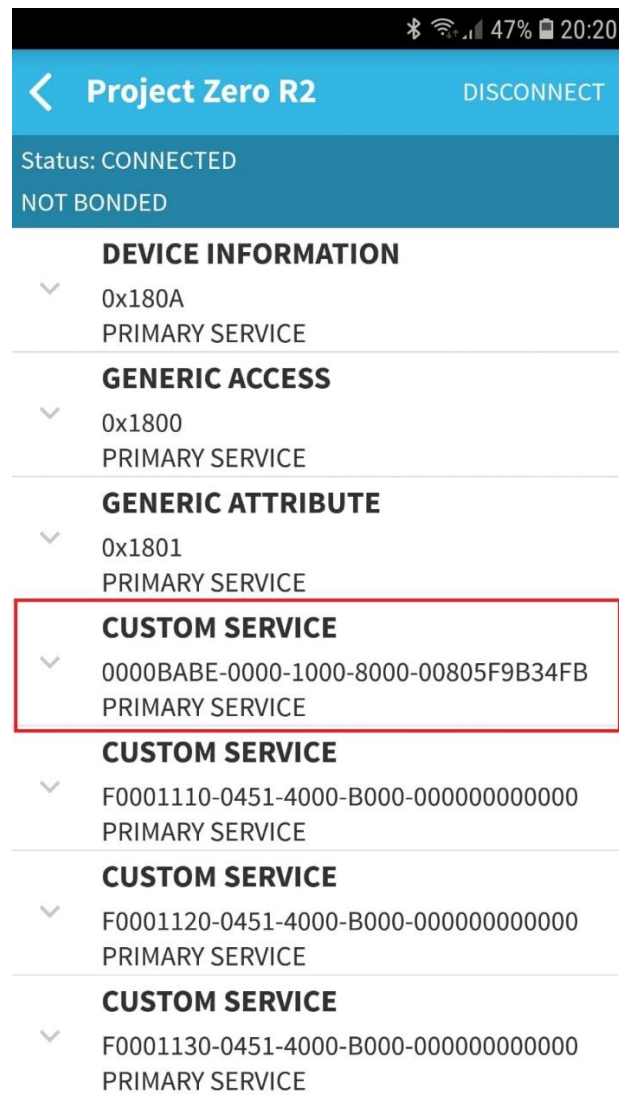


Figure 4.3 BLE Scanner app – Custom Service 0xBABE

This service is basically created for reading the voltage value read from the ADC. It has two characteristics, one for voltage and the other for the current. However, since we are only verifying the BLE data communication, only the voltage characteristic will be under consideration here.

The idea is to first read a zero value by merely connecting the ground pin to the analog pin by a jumper cable. The expected value will be, of course, very close to 0V as the range of the voltage in this project is between 0V and 60V.

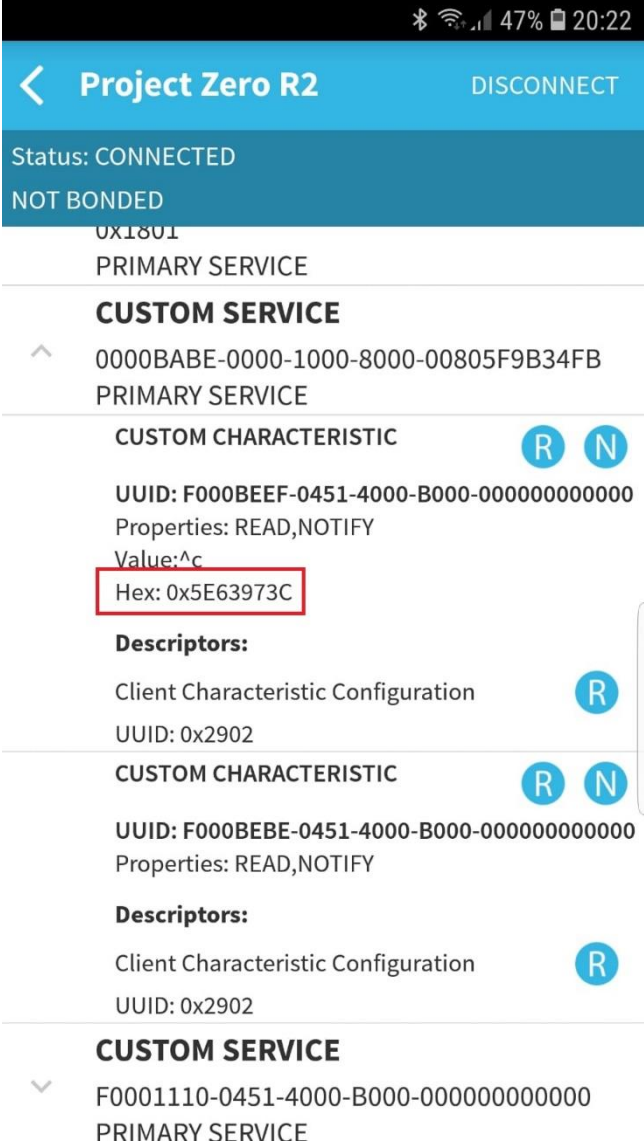


Figure 4. 4 BLE Scanner – Voltage Char 0xBEEF - 0V check

As shown above, the read hexadecimal value is 0x5E63973C. According to the BLE Scanner app protocol, the data is sent in reverse order, which means that the higher bytes are written first, then comes the lower bytes. Now we can check if the value is zero or not. Actually, 0x3C97635E is 0.018V, which is very close to 0V.

Now in order to make sure of the full functionality of the ADC, we can check whether the 3.3V will be read or not by connecting the 3.3V pin to the ADC pin by a jumper cable. Of course, since 3.3V is the maximum amount of volts that can be applied and read by an ADC pin, it will correspond to the maximum amount of voltage, which should be very close to 60V.

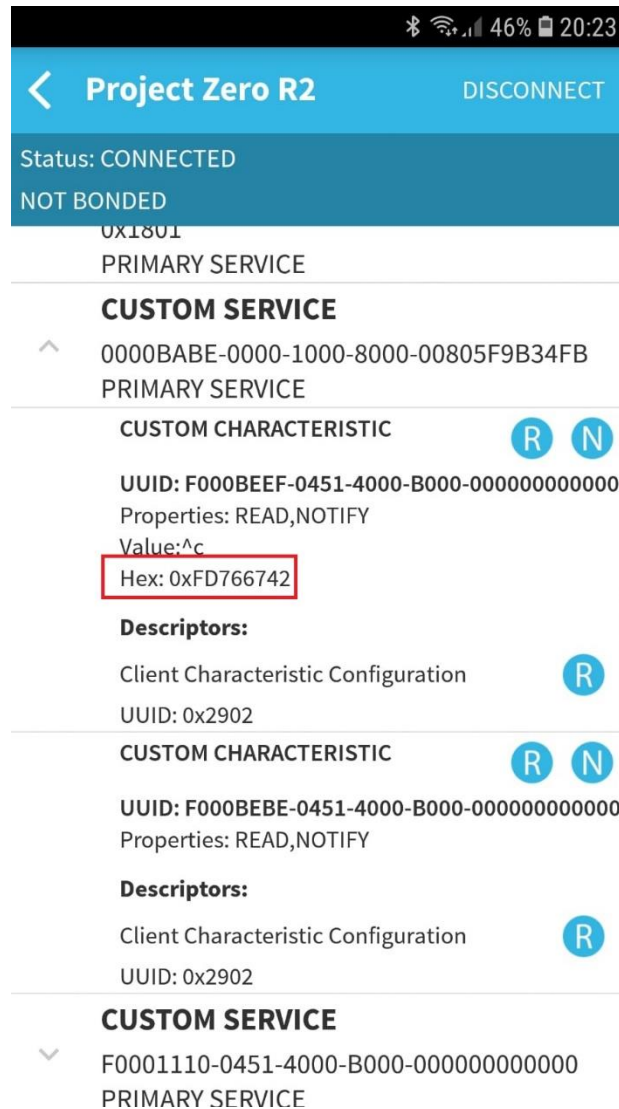


Figure 4.5 BLE Scanner - Voltage Char 0xBEEF – 3.3V check

As shown above, the read hexadecimal value is 0xFD766742. According to the BLE Scanner app protocol, the data is sent in reverse order, which means that the higher bytes are written first, then comes the lower bytes. Now we can check if the value is around 60V or not. Actually, 0x426776FD is 57.86V, which is very close to 60V.

CHAPTER V

5. Conclusion

5.1. Future Perspectives

5.1.1. HW Improvements

In such applications like ours, surge and transient protection become crucial. The protection circuit applied on the PCB should be enough for the targeted application. However, further protection can be applied as an external circuitry in order to show various immunities towards IEC61000-4-4 and IEC61000-4-5.

Furthermore, even if a further HW change is to be considered, such as using a distinct integrated component for voltage and current sensing like INA226-Q1, INA225-Q1, or LMP860x-Q1, the increased transient immunity for the high-side current sensing circuitry can be applied, as shown below.

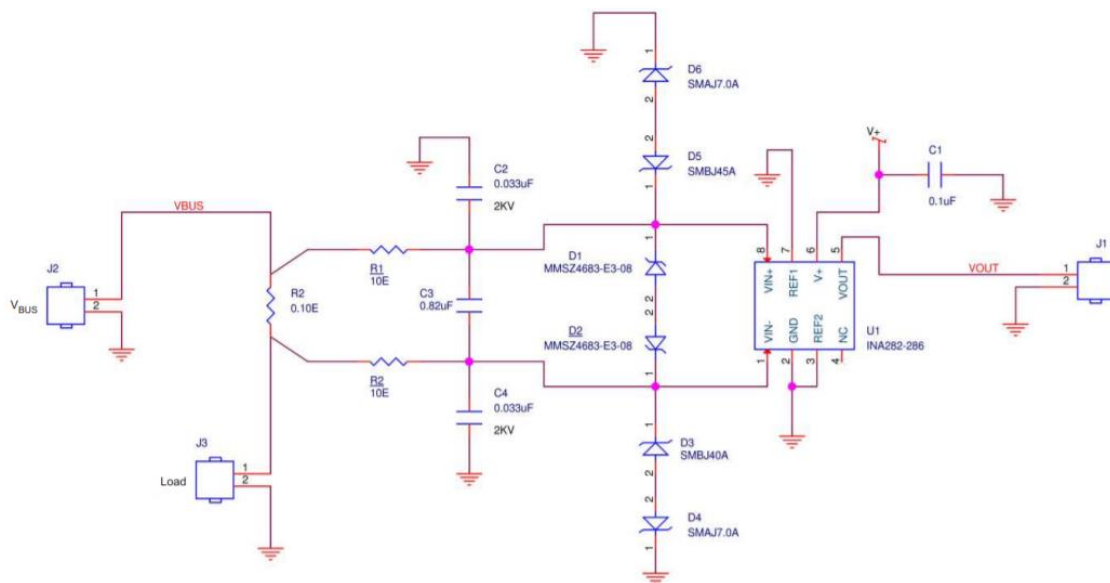


Figure 5.1 High-Side Current Sensing with Improved Transient Immunity [31]

This type of circuit can be applied not only to the battery specification sensing applications but also to many different work areas. Such as:

- PLC 24V industrial applications
- Current sensing applications with 24V
- Bi-directional motor load control
- The solar inverter applications
- Electric hybrid vehicles

Also, this high-side current sense is designed to meet the following specifications:

- Load supply with a maximum of 24 V
- Voltage protection with a maximum of 45 V
- 5V DC supply voltage
- Electrical fast transient (EFT) withstanding capability of 1KV
- Overall accuracy more than 2%

5.1.2. FW Improvements

The best improvement in terms of FW would be related to the situations when the device itself is not connected to Bluetooth, in other words, when the device is offline. Not always does a user have a chance to have the proper Bluetooth connection. However, the user may want to learn about the battery specs even though there is no Bluetooth connection at that time.

For this improvement, an algorithm can be applied which allows us to store the acquired data in flash memory. After collecting the data inside the flash, they can be sent to the BLE app as soon as the Bluetooth connection is established. This is a possible improvement since the HW design includes a flash memory implemented on the PCB.

Starting from a fixed acquisition duration period, the amount of flash memory can be calculated using the following formulas, with an example acquisition period of 24 hours and considering the average time of voltage and current acquisition to be approximately 20ms and two temperature values are sent after 30 correct acquisitions and considering that every sample is 16 bits.

$$acq_{time} = 30 \cdot 20ms = 600ms \quad (5.1)$$

$$acq_{size} = 2 \cdot (30 \cdot 16bit) + (2 \cdot 16bits) = 124 \text{ byte} \quad (5.2)$$

$$\#acq = \frac{24h}{600ms} = 144000 \quad (5.3)$$

$$memorySize = 124byte \cdot 144000 \approx 17.028 \text{ MByte} \quad (5.4)$$

So we can easily deduct that a simple flash memory with 32 Mbyte storage value should be more than enough for the desired application.

5.1.3. Cloud Computing

Cloud computing for battery specs management can be beneficial. It basically includes data storage and data computing.



Figure 5. 2 Cloud computing connecting many stations

By implementing cloud computing, we will be able to connect many devices to communicate with each other. This simply implies that there will be a lot more than a single data pack for us in order to compute the required SoC and SoH values. Since there will be many devices and many users will be contributing, the SoC and SoH values will be more accurate.

Apart from that, also using the internet, it will be possible to gather all the data from the devices that are connected to our device itself, which means that we will be collecting some valuable data from many different batteries or alternators.

5.2. Conclusion

The main idea of this thesis work was simply to improve the original BATMAN project by designing and developing both hardware and firmware in order to measure the voltage, the current, and the temperature and, as a result, calculate and send the related SoC and SoH of lead-acid batteries.

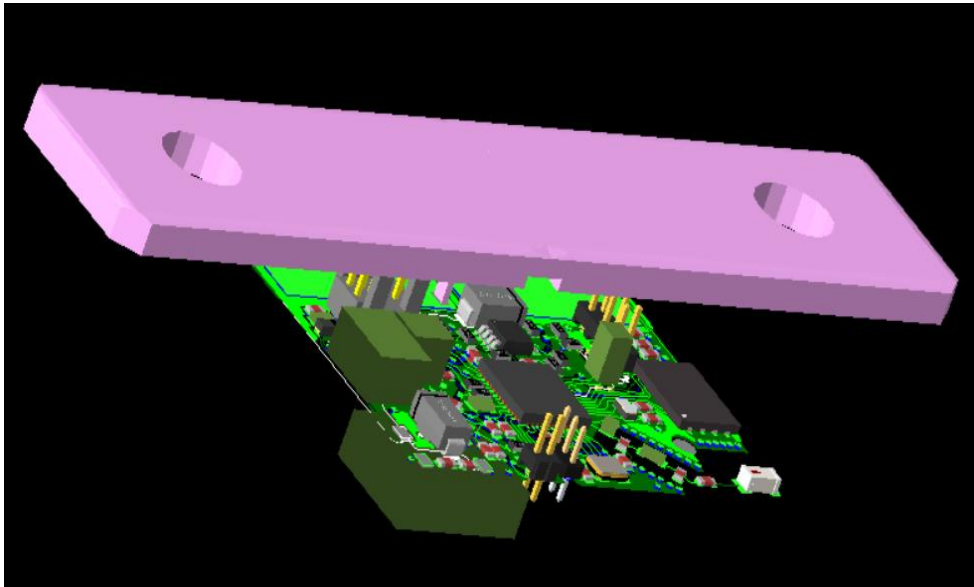


Figure 5. 3 3D top view

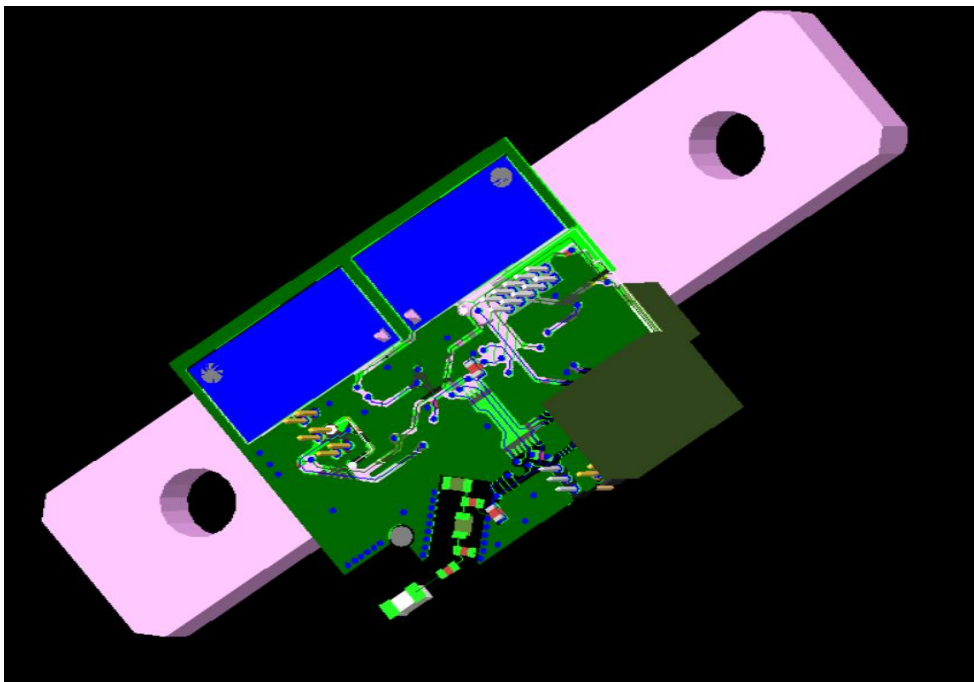


Figure 5. 4 3D bottom view

In order to complete this work, the starting point was to identify all the necessary requirement points. After understanding and observing all the needs, a hardware design has been done by respecting many PCB design rules in order to keep the work clean and safe for operating conditions.

Since we use a shunt resistor with a case, the design can be considered as very robust to external disturbances such as heat, dust, etc. That makes the device very useful for industrial applications, especially when considering that the device is entirely meant to be mounted on the batteries that are generally inside the related vehicle.

The device is able to sense the voltage, current, and temperature parameters accurately, thanks to the design and the sensors used. However, the primary purpose is to calculate SOC and SoH and let the user know about them. In this manner, a suitable algorithm is needed to be used in the firmware. At that point, the algorithm provided by the *brainTechnologies* is beneficial for the firmware development in order to estimate the required SoC and SoH values as accurate as possible.

We can easily say that, in the near future, the vehicles working with fuel will be replaced by either fully electric vehicles or hybrid models. In any case, battery management will be crucial for the systems since the only electricity that the vehicle will need comes from the battery itself. Even this thesis work can be extended to the very limits because even one cell of a battery is fundamental to be monitored and get information about in order to take actions before facing and failures and charge imbalances.

In conclusion, by respecting the initial requirements of the whole project, hardware and a firmware design for a device have been done in order to estimate the parameters of interest, which can lead the related products or ideas on either the current and future market applications or future research works.

Bibliography

- [1] T. Flaim, Y. Wang, R. (. A. C. Mercado, N. Kaiser ve H. A. MacLeod, «"High-Refractive Index Polymer Coatings for Optoelectronics Applications". SPIE Proceedings of Optical Systems Design. Advances in Optical Thin Films,» 2004.
- [2] MIT ve Electric Vehicle Team, «A Guide to Understanding Battery Specifications,» 2012.
- [3] S.Pregolato, «Real-Time Battery Conditions Estimation - Energetic framework definition and algorithm implementation for real-time determination of the batteries' SoC and SoH,» *M.S. Thesis Politecnico di Torino*, October 2018.
- [4] C. Zhang, S. Mcloone, K. Li ve Z. Yang, «Battery modelling methods for electric vehicles,» June 2014.
- [5] D. Di Domenico, G. Fiengo ve A. Stefanopoulou, «Lithium-ion battery state of charge estimation with a kalman filter based on an electrochemical models in Control Applications,» %1 içinde *IEEE International Conference*, 2008.
- [6] K. Takano, K. Nozaki, Y. Saito, A. Negishi, K. Kato ve Y. Yamaguchi, «Simulation study of electrical dynamic characteristics of lithium-ion battery,» *Journal of Power Sources*, cilt 2, no. 90, pp. 214-223, 2000.
- [7] M. Murnane ve A. Ghazel, «A Closer Look at State of Charge (SOC) and State of Health (SOH) Estimation Techniques for Batteries,» *Analog Devices*, 2017.
- [8] H. Group, «Intelligent battery sensor (IBS),» [Online]. Available: <https://www.hella.com/mining/en/Intelligent-Battery-Sensor-1356.html>. [Accessed: 14 12 2020].
- [9] BOSCH, [Online]. Available: <https://www.bosch-mobility-solutions.com/en/products-and-services/passenger-cars-and-light-commercial-vehicles/interior-and-body-systems/body-electronics/electronic-battery-sensor/>. [Accessed: 14 12 2020].
- [10] C. AG, «Continental Intelligent Battery Sensor (IBS),» [Online]. Available: <https://www.continental-automotive.com/en-gl/Trucks-Buses/Vehicle-Chassis-Body/Advanced-Sensors/Intelligent-Battery-Sensor>. [Accessed: 14 12 2020].
- [11] F. Di Fazio ve D. Fazi, *Current and Voltage Sensing Circuit for Automotive Batteries SoH and SoC Determination*, Torino: MSc Thesis Politecnico di Torino, December 2019.
- [12] N. Technologies, «Current Sensing Theory,» [Online]. Available: <https://www.nktechnologies.com/engineering-resources/current-sensing-theory/>. [Accessed: 20 12 2020].
- [13] P. Analog, «Why Use Current Shunt Monitors?,» 24 February 2009. [Online]. Available: <https://www.planetanalog.com/why-use-current-shunt-monitors/>.

- [Accessed: 12 December 2020].
- [14] K. Maniar, «Comparing shunt- and hall-based isolated current-sensing,» 8 November 2019. [Online]. Available: ti.com/lit/an/sbaa293b/sbaa293b.pdf. [Accessed: 21 December 2020].
- [15] TexasInstruments, «Automotive Shunt-Based ± 500 -A Precision Current Sensing Reference Design,» February 2017. [Online]. Available: <https://www.ti.com.cn/cn/lit/ug/tiducj6/tiducj6.pdf>. [Accessed: 28 December 2020].
- [16] ElectronicsTutorials, «MOSFET as a Switch,» [Online]. Available: https://www.electronics-tutorials.ws/transistor/tran_7.html. [Accessed: 28 December 2020].
- [17] MaximIntegrated, «Application Note 751: Linear Regulators in Portable Applications,» 2002. [Online]. Available: <https://www.maximintegrated.com/en/design/technical-documents/tutorials/7/751.html>. [Accessed: 28 December 2020].
- [18] TexasInstruments, «LMR16006 SIMPLE SWITCHER® 60 V 0.6 A Buck Regulators With High Efficiency ECO Mode,» October 2014. [Online]. Available: <https://www.ti.com/lit/ds/symlink/lmr16006.pdf>. [Accessed: 28 December 2020].
- [19] TexasInstruments, «INA226-Q1 AEC-Q100, 36-V, 16-Bit, Ultra-Precise, I2C Output Current, Voltage, and Power Monitor with Alert,» May 2020. [Online]. Available: <https://www.ti.com/lit/ds/symlink/ina226-q1.pdf>. [Accessed: 29 December 2020].
- [20] S. Kal, Basic Electronics: Devices, Circuits, and IT fundamentals, Prentice-Hall of India Pvt Ltd., 2004.
- [21] B. Kuo ve F. Golnoraghi, Automatic Control Systems, New York: NY: Wiley, 2003.
- [22] G. Palumbo ve S. Pennisi, Feedback amplifiers: theory and design, Boston/Dordrecht/London: Kluwer Academic, 2002.
- [23] Etechnog, «Applications, Advantages, Disadvantages of Differential Amplifier,» 2018. [Online]. Available: <https://www.etechnog.com/2019/05/applications-differential-amplifier.html>. [Accessed: 29 December 2020].
- [24] Vishey, «Power Metal Strip® Battery Shunt Resistor W/Molded Enclosure Very Low Value (50 $\mu\Omega$, 100 $\mu\Omega$, 125 $\mu\Omega$, and 500 $\mu\Omega$),» 1 January 2019. [Online]. Available: <https://www.vishay.com/docs/31094/wsbm8518.pdf>. [Accessed: 29 12 2020].
- [25] TexasInstruments, «CC2640R2F-Q1 SimpleLink™ Bluetooth,» January 2017. [Online]. Available: <https://www.ti.com/lit/ds/symlink/cc2640r2f-q1.pdf>. [Accessed: 29 December 2020].
- [26] TexasInstrument, «2.4-GHz Inverted F Antenna,» April 2007. [Online]. Available: <https://www.ti.com/lit/an/swru120d/swru120d.pdf>. [Accessed: 30

December 2020].

- [27] JohansonTechnology, «High Frequency Ceramic Solutions 2450AT18A100,» 07 Spetember 2018. [Online]. Available:
<https://www.johansontechnology.com/datasheets/2450AT18A100.pdf>.
[Accessed: 30 December 2020].
- [28] TexasInstruments, «General RTOS Concepts,» [Online]. Available:
https://dev.ti.com/tirex/explore/node?node=AHxv--RBRKmEZioO0JEGGA_krol.2c__LATEST. [Accessed: 04 January 2021].
- [29] TexasInstruments, «Sensor Controller Studio,» [Online]. Available:
<https://www.ti.com/tool/SENSOR-CONTROLLER-STUDIO>. [Accessed: 05 January 2021].
- [30] TexasInstrument, «LAUNCHXL-CC2640R2,» 06 February 2019. [Online]. Available:
<https://www.ti.com/lit/ml/swru500b/swru500b.pdf?ts=1610672873831>.
[Accessed: 15 January 2021].